



Norwegian University of  
Science and Technology

# Plasma Instabilities in Electron-Positron Pair Beams from Blazars

**Martin Hornkjøl**

MSc in Physics

Submission date: May 2018

Supervisor: Michael Kachelriess, IFY

Norwegian University of Science and Technology  
Department of Physics



# Abstract

The non-detection of an electromagnetic cascade in the electron-positron plasma beams from blazars has led many physicists to invoke an intergalactic magnetic field that deflects charged particles away from our field of view. In this thesis we look at a different explanation. Namely that the beams lose their energy through plasma instabilities rather than the inverse Compton scattering which would create the cascade. We use a covariant formalism to calculate the linear response tensor of the plasma. Using this tensor we find the absorption coefficient for particles distributed according to the Jüttner distribution and for a different distribution based on simulations. The absorption coefficient is found to diverge for specific values of the phase velocity when the electric field of the mode vanishes. This is unphysical, which means there is some issue with the calculations. The issue is identified as the assumption that the imaginary part of the frequency, known as the absorption coefficient, is small. This assumption contradicts the results making the calculations invalid. To solve this problem one would have to redo the calculations avoiding this assumption.



# Sammen drag

Mangelen på en elektromagnetisk kaskade i elektron-positron plasma stråler fra blasarer har fått mange fysikere til å foreslå at de ladete partiklene blir ledet vekk fra vårt synsfelt av et intergalaktisk magnetisk felt. I denne oppgaven ser vi på en annen forklaring. Vi ser på muligheten for at strålene taper energien deres på grunn av ustabilitet i plasma isteden for den inverse Compton spredningen som ville produsert kaskaden. Vi bruker en kovariant formalisme til å regne ut den lineære respons tensoren til plasmaet. Ved å bruke denne tensoren så finner vi absorpsjonskoeffisienten for partikler fordelt i henhold til Jüttner fordelingen og for en annen fordeling basert på simuleringer. Vi finner ut at absorpsjonskoeffisienten divergerer for visse verdier av fase hastigheten som koresponderer til at det elektriske feltet i moden blir null. Dette er ikke fysisk, noe som betyr at det er et problem med utregningene. Vi identifiserer at problemet kommer fra en antagelse om at den imaginære delen av frekvensen, kjent som absorpsjonskoeffisienten, er liten. Dette motsier resultatet som viser at den er uendelig. For å løse dette problemet må man gjøre utregningene på nytt uten å gjøre antagelsen.



# Preface

This thesis was completed in the spring of 2018 as part of my master's degree in physics. It is written for the Division of Theoretical Physics at the Department of Physics at NTNU. I want to sincerely thank my supervisor Prof. Michael Kachelriess for taking me on as a student and for his invaluable guidance in last two years. I also want to thank my fellow students Nicolai Gerrard, Stian T. H. Hartman and Jonas L. Willadsen for freely exchanging ideas related and unrelated to our theses and general companionship as well as Erik Liodden for helping me optimize my Python scripts.





# Contents

<b>1</b>	<b>Introduction</b>	<b>1</b>
<b>2</b>	<b>Active Galactic Nuclei and Quasars</b>	<b>5</b>
2.1	Structure of an AGN . . . . .	5
2.2	The unified AGN model . . . . .	7
<b>3</b>	<b>Plasmas and Instabilities</b>	<b>9</b>
3.1	Plasmas . . . . .	9
3.2	Plasma Instabilities . . . . .	12
<b>4</b>	<b>Covariant Plasma theory</b>	<b>15</b>
4.1	Special Relativity and Covariant Formalism . . . . .	15
4.2	Covariant Plasma Theory . . . . .	16
4.3	Wave Energetics and the Absorption Coefficient . . . . .	18
<b>5</b>	<b>The Linear Response Tensor</b>	<b>21</b>
5.1	The Weak-Turbulence Expansion . . . . .	21
5.2	Lagrangian Density . . . . .	22
5.3	Forward-Scattering Method . . . . .	22
5.4	Jüttner Distribution . . . . .	25
5.5	The Relativistic Plasma Dispersion Function . . . . .	25
5.6	Instability Due to an Anisotropic Strictly-Parallel Thermal Distribution	26
<b>6</b>	<b>Absorption Coefficient for the Jüttner Particle Distribution</b>	<b>29</b>
6.1	Absorption Coefficient for the Jüttner Distribution . . . . .	29
6.2	Alternative Absorption Coefficient for the Jüttner Distribtuion . . . . .	35
<b>7</b>	<b>Absorption Coefficient for a Simulatied Particle Distribution</b>	<b>39</b>
7.1	Absorption Coefficient for Simulated Distribution Function . . . . .	39
7.2	The Distribution Function . . . . .	47
<b>8</b>	<b>Summary and Conclusion</b>	<b>49</b>
<b>A</b>	<b>MacDonald functions</b>	<b>51</b>
<b>B</b>	<b>Derivatives</b>	<b>53</b>
B.1	Derivatives of the Relativistic Particle Distribution Function . . . . .	53
B.2	Derivatives of $I(z)$ for $z < 1$ . . . . .	54
B.3	Derivatives of $I(z)$ for $z > 1$ . . . . .	57



# List of Figures

1.1	The quasar M87 with its accompanying jet extending more than 5000 light years. Taken from hubblesite.org (2017). . . . .	2
1.2	The Feynmann diagrams for the two processes pair creation (left) and Compton scattering (right). . . . .	3
2.1	The unified AGN model. A black hole surrounded by an accretion disk and a torus of matter. An energy jet extends from the central source. The different types of AGN measured based on our position in regards to the AGN is indicated with arrows. Taken from Ref [16], but originally in Ref [17]. . . . .	6
3.1	An illustration of a stable system (left) and an unstable system (right).	13
6.1	The figure shows the absorption coefficient as a function of $z$ for $\rho = 0.01$ and $x = 4$ . It is positive, stable, until $z$ gets close to 1 where it becomes negative, unstable. . . . .	33
6.2	The figure shows the absorption coefficient as a function of $z$ for $\rho = 1$ and $x = 4$ . It is positive, stable, until it diverges and negative, unstable, after. . . . .	33
6.3	The figure shows the absorption coefficient as a function of $z$ for $\rho = 100$ and $x = 4$ . It is positive, stable, for very small values of $z$ then it diverges and becomes negative, unstable, before it diverges again and becomes positive. . . . .	34
6.4	The figure shows $\Pi_L$ with prefactors and $R_L$ as a function of $z$ for $\rho = 1$ and $x = 4$ . One can see that $\Pi_L$ with prefactors is always positive while $R_L$ takes both positive and negative values. . . . .	34
7.1	The figure shows the absorption coefficient as a function of $z$ for $r = 0.01$ and $x_0 = 165$ . It is positive, stable, until it diverges and after the divergence it is negative, unstable. . . . .	45
7.2	The figure shows the absorption coefficient as a function of $z$ for $r = 1$ and $x_0 = 165$ . It is positive, stable, until it diverges and after the divergence it is negative, unstable. . . . .	45
7.3	The figure shows the absorption coefficient as a function of $z$ for $r = 100$ and $x_0 = 165$ . It is positive, stable, until it diverges and after the divergence it is negative, unstable. . . . .	46
7.4	The figure shows $\Pi_L$ with prefactors (left) and $R_L$ (right) as a function of $z$ for $r = 1$ and $x_0 = 165$ . One can see that $\Pi_L$ with prefactors is positive while $R_L$ is both positive and negative. . . . .	46

7.5	Plots of the data points from the simulations using ELMAG [22]. It shows the spectrum of the first generation of $e^+e^-$ pairs in an electromagnetic cascade on the extragalactic background light. The left graph is plotted with logarithmic axis and the right graph is plotted with linear axis. Note that some data points are missing in each graph. The logarithmic graph are missing the data points which have a zero value on the y-axis. The linear graph is missing some data points at the high energy. . . . .	47
7.6	The figure shows the simulated data points of the distribution of particles over energy with the approximation function giving an analytic expression for it. . . . .	48
A.1	The first 4 orders of the Bessel function of the first (right) and second (left) kind. . . . .	51
A.2	The first 4 orders of the modified Bessel function of the second kind. .	52

# List of Tables

2.1	A table of the different types of AGN's sorted by their optical emission line properties and their radio-loudness. NLRG and BLRG are narrow and broad line radio galaxies, SSRQ and FSRQ are steep and flat spectrum radio quasars, QSO are quasi-stellar object and FR I and FR II are Fanaroff-Riley Type 1 and 2 radio galaxies. Taken from Ref [17]. . . . .	8
-----	--	---



# Conventions, Variables and Abbreviations

## Conventions

Kronecker Delta

$$\delta^\mu_\nu = \begin{cases} 1 & \text{if } \mu = \nu \\ 0 & \text{otherwise} \end{cases} \quad (1)$$

Step function

$$H(x) = \begin{cases} 1 & \text{if } x > 0 \\ 0 & \text{if } x < 0 \end{cases} \quad (2)$$

Metric tensor in flat spacetime

$$\eta_{\alpha\beta} = \begin{pmatrix} 1 & 0 & 0 & 0 \\ 0 & -1 & 0 & 0 \\ 0 & 0 & -1 & 0 \\ 0 & 0 & 0 & -1 \end{pmatrix}, \quad (3)$$

The wave amplitude is defined as  $\delta A = \sum_{\mathbf{k}} A_{\mathbf{k}} \exp(-(i\mathbf{k} \cdot x - i\omega t))$  such that a absorption coefficient  $\gamma$  smaller than zero makes the plasma unstable.

## Abbreviations

- AGN** - Active galactic nucleus
- EBL** - Extragalactic background light
- EM** - Electromagnetic
- EoM** - Equation of Motion
- ICC** - Inverse compton cascade
- IGM** - Intergalactic medium
- IGMF** - Intergalactic magnetic field
- LRT** - Linear response tensor
- RPDF** - Relativistic plasma dispersion relation

Variables	
$z$	Phase velocity
$\beta$	Beam velocity
$n$	Beam number density
$n_{\text{pr}}$	Proper beam number density
$n_0$	Background number density
$\rho$	$m/T$
$m$	Electron mass
$q$	Electron charge
$\epsilon_0$	Vacuum permittivity
$\mu_0$	Vacuum permeability
$\gamma$	Absorption coefficient or Lorentz factor
$\omega$	Frequency
$k$	Wave number
$\omega_p$	Plasma frequency with density $n$
$\omega_{p,0}$	Plasma frequency with density $n_0$
$\omega_L$	Frequency of the longitudinal wave mode
$x$	$\omega_p/\omega_L$
$x_0$	$\omega_{p,0}/\omega_L$
$\lambda_D$	Debye length
$\Lambda$	Plasma parameter



# 1 — Introduction

This thesis will look at the growth rate of plasma instabilities in electron-positron pair beams in relativistic energy jets from blazars. A covariant description of plasma theory will be introduced and used to calculate the response tensor of the plasma, from which we can find the growth rate for a specific particle distribution function. Two distribution functions will be looked at: First the Jüttner distribution and then a more complicated distribution function based on a simulation of the beam. The goal of the thesis is to confirm or disagree with, dependent on the results, the conclusions drawn by Supsar in his dissertation and in the articles of Schlickeiser et. al. that the energy jets dissipate their energy into the cosmic voids before they can create an electromagnetic cascade via inverse Compton scattering [1, 2, 3]. Thereby making an intergalactic magnetic field (IGMF) unnecessary to explain the non-detection of the aforementioned cascade by gamma-ray telescopes.

Magnetic fields are found everywhere in the universe where we have the means of detecting them, and are thought to be created by the amplification of existing magnetic fields by dynamo and compression mechanisms. These mechanisms requires a non-zero magnetic field to be present and act as a seed-field to be amplified [4]. This seed-field has to be generated independently by a mechanism that stems from the time before or at the time of structure formation [4]. The origin of this seed-field and its strength is one of the important, unsolved, problems of cosmology. Its detection and measurement is easiest in galaxies and other areas that contain radiating objects, but the magnetic fields measured from these structures are distorted by plasma effects and magnetohydrodynamics [4]. As we do not know exactly how the magnetic field is affected by these complicated effects, we cannot use these measurements to predict the strength of the original seed-fields [4]. These seed-fields can only be found, in their original form, in the intergalactic medium (IGM) in cosmic voids where there should be no plasma or other effects to disturb it. Here they are, however, difficult to observe, though one way of detecting them could be to look at how energy jets from quasars are affected by their passage through it.

Quasars are a subgroup of active galactic nuclei defined by their high luminosity and a small size of less than  $\sim 7''$  [5]. These energetic objects are found in the center of galaxies and are most likely powered by supermassive black holes, with a masses of about  $10^8 M_{\odot}$ , accreting several  $M_{\odot}$  of mass a year. The mass falling into the black hole forms a mostly two dimensional accretion disk and gives the quasar a luminosity equalling  $10^{12}$  suns. Figure 1.1 shows the quasar M87 in the near-infrared spectrum taken with HST's Wide Field and Planetary Camera. Quasars can be divided into two subgroups, namely radio-loud and radio-quiet, depending on their emission of radio waves.

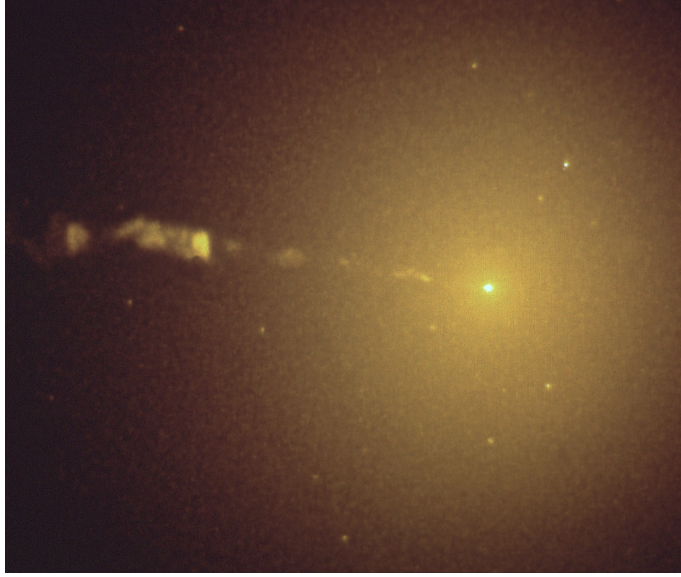


Figure 1.1: The quasar M87 with its accompanying jet extending more than 5000 light years. Taken from [hubblesite.org](http://hubblesite.org) (2017).

Radio-loud quasars emit an energy jet of high energy light rays perpendicular to their accretion disk. If this jet happens to be pointing at the earth the quasar is called a blazar. The  $\gamma$ -ray Cherenkov Telescopes H.E.S.S., MAGIC and VERITAS and the Fermi LAT have discovered about 50 blazars emitting jets with energies in the TeV range [2]. Gamma rays of these energies cannot propagate over cosmological distances as they will interact with the photons of the extragalactic background light (EBL) and create electron-positron pairs through pair creation [6]  $\gamma + \gamma' \rightarrow e^- + e^+$  as seen in 1.2. This process is possible if  $E_\gamma E_{\gamma'}(1 - \cos \theta) > 2m_e^2 c^4$ . This expression is found from conservation of four-momentum

$$\begin{aligned} (p_\gamma + p_{\gamma'})^2 &= (p_{e_1} + p_{e_2})^2 \\ p_\gamma^2 + p_{\gamma'}^2 + 2p_\gamma \cdot p_{\gamma'} &= p_{e_1}^2 + p_{e_2}^2 + 2p_{e_1} \cdot p_{e_2} \\ 2(E_\gamma E_{\gamma'} - \mathbf{p}_\gamma \cdot \mathbf{p}_{\gamma'}) &= 2m_e^2 c^4 + 2(E_{e_1} E_{e_2} - \mathbf{p}_{e_1} \cdot \mathbf{p}_{e_2}). \end{aligned} \quad (1.1)$$

In the center of mass frame of the electrons the momenta are  $p_{e_1} = (E_1, \mathbf{p})$  and  $p_{e_2} = (E_2, -\mathbf{p})$ . Since the photons are massless their energy is related to momentum by  $E = |\mathbf{p}|c$ . With this (1.1) becomes

$$\begin{aligned} 2(E_\gamma E_{\gamma'} - E_\gamma E_{\gamma'} \cos \theta) &= 2m_e^2 c^4 + 2m_e^2 c^4 + 2|\mathbf{p}|^2 + 2|\mathbf{p}|^2 \\ E_\gamma E_{\gamma'}(1 - \cos \theta) &> 4m_e^2 c^4. \end{aligned} \quad (1.2)$$

With a maximum energy of the extragalactic background light of 13.6 eV the minimum energy for the reaction is about  $7 \cdot 10^{10}$  eV. These electron-positron pairs propagate in the intergalactic medium in the cosmic voids where it has been thought that the electrons and positrons inverse Compton scatter off the EBL,  $e^- + \gamma \rightarrow e^- + \gamma'$  as seen in Figure 1.2, to create photons [7] with energies of 100 GeV [2] that can again pair produce  $e^+ e^-$  pairs. This will happen multiple times causing an electromagnetic inverse Compton cascade (ICC) relaxing the TeV jet to the GeV range;

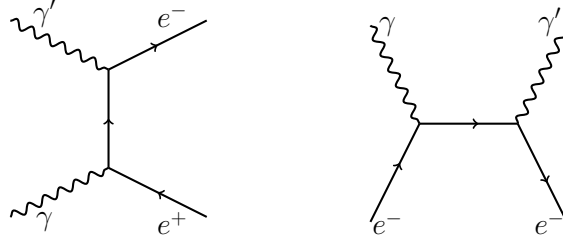


Figure 1.2: The Feynmann diagrams for the two processes pair creation (left) and Compton scattering (right).

however, this cascade has not been detected.

The lack of observations of an electromagnetic cascade suggest some process is hindering it or its detection and has been used as evidence of an IGMF [8, 9, 10, 11, 12]. A strong IGMF, with  $B > 10^{-16}$  Gauss, could deflect the charged electrons and positrons away from the line of sight of the observer [8]. This would explain the non-detection of the ICC.

A different process explaining the non-observation of the ICC was proposed by Chang et. al., based on the fact that the charged particles in the jet is a plasma and is therefore inclined towards instabilities [13]. This was also discussed by Schlickeiser, Supsar et al. [3]. Later Supsar concluded in his dissertation that two-stream instabilities, mainly the oblique electrostatic instability, would cause the free energy in the plasma to dissipate into the IGM disallowing the ICC from occurring in the first place. He did this using the kinetic theory of plasma instabilities for relativistic speeds.

In this thesis we will calculate instabilities for the longitudinal mode. We will use a covariant plasma theory, following Donald Melrose [14], to find a linear response tensor (LRT) for a plasma with a certain distribution function. With this LRT we can find an absorption coefficient whose sign determines the stability of the plasma. This thesis is divided into 8 chapters including the introduction. The second chapter introduces the physics behind AGN's and their classifications. The third chapter presents and defines the fundamentals of classical plasma theory and instabilities. In chapter four we define a covariant plasma theory and derive expressions for its fundamentals such as the wave equation and more importantly the absorption coefficient following Ref [14]. Chapter five calculates the LRT for a Jüttner particle distribution also following Ref [14]. In chapter 6 we calculate an original expression for the absorption coefficient based on the LRT from chapter 5. Another LRT from Ref [15] is also calculated in this chapter. Using a new particle distribution function based on simulations, an original LRT and absorption coefficient, based on the LRT in Ref [15], is calculated in chapter 7. Finally, chapter 8 summarizes and concludes the results. The thesis ends with two appendices A and B discussing Bessel functions and cataloging derivatives too unhandy to include in the main text, respectively.



## 2 — Active Galactic Nuclei and Quasars

The core of some galaxies is so luminous that it outshines the rest of the galaxy. These galaxies are called active galaxies and their centers are called active galactic nuclei (AGN). There are many subgroups of active galactic nuclei, the two largest being Seyfert galaxies and quasars. The difference between these two subgroups are somewhat arbitrary, with Seyfert galaxies emitting energy comparable to all the stars in the galaxy ( $\sim 10^{11} L_{\odot}$ ) and quasars emitting up to 100 times as much. A blazar is again a subgroup of radio-loud quasars with an energetic jet pointing towards the observer. In this section all calculation will be in cgs units.

### 2.1 Structure of an AGN

An AGN consists of a supermassive black hole at the center of a galaxy. The black hole is accreting mass. The mass falling into the black hole forms a mostly two-dimensional disk known as an accretion disk. The accretion disk contains mostly ionized material and a lot of energy is created by its absorption into the black hole giving the AGN its large luminosity. The accretion disk extends for several hundred Schwarzschild radii forming the central region of the AGN. This central region of the AGN is surrounded by a torus of matter with an inner diameter of  $\sim 1.5$  pc and an outer diameter of  $\sim 30$  pc. AGN's can be radio-loud or radio-quiet depending on the amount of radiation they emit in the radio-spectrum. Radio-loud quasars also emit jets. Jets are linear structures of plasma moving from the center of the quasar, normal to the plane of the accretion disk, at relativistic speeds. Figure 2.1 shows the general structure of an AGN [16]. By simple calculations one can estimate the mass and fueling of a quasar. This will be done here following Ref [5]. The mass of the center of a quasar can be approximated by noting that the outward radiation pressure must be balanced by an inward gravitational force. Otherwise the quasar would disintegrate. Let us do the calculation for a completely ionized hydrogen gas. Assuming Euclidean geometry the energy flux of the quasar is

$$F = \frac{L}{4\pi r^2}, \quad (2.1)$$

where  $L$  is the luminosity (energy per time). In the same way that the momentum carried by a photon is  $E/c$  the momentum flux is  $P_{\text{rad}} = \frac{F}{c} = \frac{L}{4\pi r^2 c}$ . The outward radiation force of a single electron is obtained by multiplying the momentum flux with the cross section for an interaction with a photon

$$\mathbf{F}_{\text{rad}} = \sigma_e \frac{L}{4\pi r^2 c} \hat{\mathbf{r}}, \quad (2.2)$$

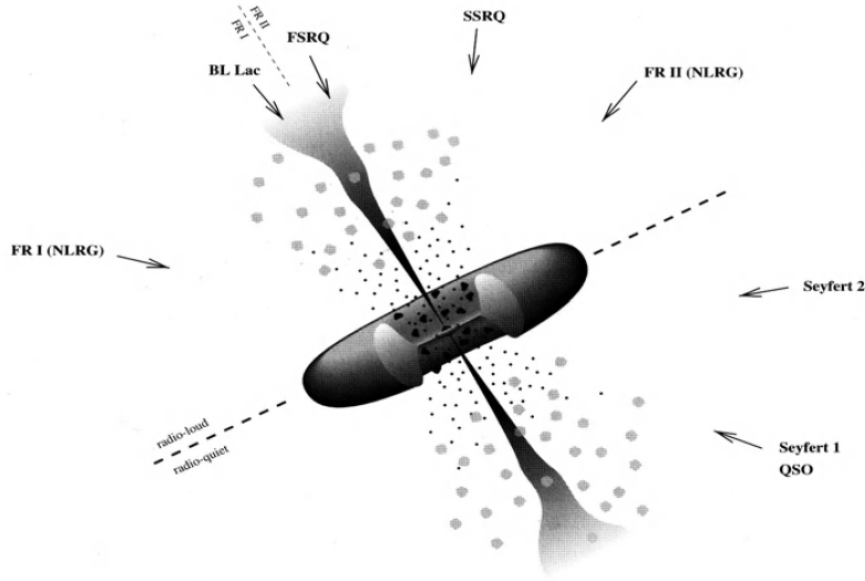


Figure 2.1: The unified AGN model. A black hole surrounded by an accretion disk and a torus of matter. An energy jet extends from the central source. The different types of AGN measured based on our position in regards to the AGN is indicated with arrows. Taken from Ref [16], but originally in Ref [17].

where  $\sigma_e = 6.65 \cdot 10^{-25} \text{cm}^2$  is the Thomson scattering cross section [18]. Thomson scattering is the low energy scattering of electromagnetic radiation by a charged particle. The gravitational force on an electron-proton pair is

$$\mathbf{F}_{\text{grav}} = -\frac{GM(m_p + m_e)\hat{\mathbf{r}}}{r^2} \approx -\frac{GMm_p\hat{\mathbf{r}}}{r^2}. \quad (2.3)$$

Now, in order for the core of the quasar to stay intact, the gravitational force must be stronger or equal to that of the radiation force. That is

$$\begin{aligned} |\mathbf{F}_{\text{rad}}| &\leq |\mathbf{F}_{\text{grav}}| \\ \frac{\sigma_e L}{4\pi cr^2} &\leq \frac{GMm_p}{r^2} \\ L &\leq \frac{4\pi Gcm_p}{\sigma_e} M \approx 1.26 \cdot 10^{38} (M/M_\odot) \text{ erg/s}. \end{aligned} \quad (2.4)$$

This equation is known as the Eddington limit and  $L$  is the Eddington luminosity  $L_E$ . The equation can be used to estimate the mass of the quasar. The Eddington mass is

$$M_E = \frac{L_E}{1.26 \cdot 10^{38} \text{ erg/s}} M_\odot \approx 10^8 M_\odot \text{ g} \quad (2.5)$$

for a regular quasar of luminosity  $L \approx 10^{46} \text{ erg/s}$ .

The energy of the nucleus of a quasar is supplied by the conversion of mass to energy. This conversion is done with some efficiency  $\eta$ . The total energy available is  $E = \eta Mc^2$ . Energy is emitted at a rate  $L = dE/dt$  from the nucleus giving

$$L = \eta \dot{M} c^2, \quad (2.6)$$

where  $\dot{M} = dM/dt$  is the rate of mass accretion. The Eddington mass accretion is

$$\dot{M}_E = \frac{L_E}{\eta c^2} = \frac{0.2}{\eta} M_\odot \text{ yr}^{-1}. \quad (2.7)$$

The efficiency and therefore the viability of mass accretion as a fueling mechanism for quasars is dependent on the value of  $\eta$ . We can do an estimate of this value by looking at the potential energy of a particle falling into a non-rotating black hole. The gravitational potential of a mass  $m$  a distance  $r$  from a source is  $U = -GMm/r$ . The Schwarzschild radius,  $R_S$ , is the event horizon of a black hole which is presumably at the center of a quasar. Based on our estimates for the the black hole mass the Schwarzschild radius is

$$R_S = \frac{2GM}{c^2} = 3 \cdot 10^{13} \frac{M}{M_\odot} \text{ cm}. \quad (2.8)$$

The potential energy of a particle falling to say  $5R_S$ , ignoring relativistic effects, is

$$\frac{GMm}{5R_S} = \frac{GMn}{10GM/c^2} = 0.1mc^2 \quad (2.9)$$

suggesting that  $\eta \approx 0.1$ . With this efficiency the Eddington mass accretion becomes

$$\dot{M}_E = 2 \cdot M_\odot \text{ yr}^{-1}. \quad (2.10)$$

This calculation shows that a black hole would not have to absorb more than a couple of solar masses a year in order to fuel the quasar.

## 2.2 The unified AGN model

There are as mentioned many different types of AGN's such as quasars, Syfert galaxies, blazars and so on. The main AGN types are listed in t Table 2.1. They are classified as either radio-loud or radio-quiet. A quasar is radio-loud if the radio flux is 10 times larger than the optical B band flux. This definition makes about 10% – 15% of all AGN's radio-loud. They are also classified by their line properties, that is their emission of broad and narrow emission lines in the optical spectrum. The broad lines comes from the accretion disk while the narrow lines originates in the outlying torus. These regions emit different lines because of the different speeds of the matter in the region. Type 1 AGN's have a broad emission line, Type 2 a narrow, and emission lines are weak or absent in Type 0. It is believed that the line properties of the optical emission is directly related to the angle between the AGN jet and the observer. Type 2 have the largest angle and Type 0 the smallest. It is unknown why some AGN's are radio-loud and some radio-quiet. Some theories are that it is caused by the type of galaxy (elliptical or spiral) or that it has to do with the spin of the black hole [16]. A unified model assumes that all AGN's have the same structure described in the previous section and the difference in measurements of different AGN's comes from our spacial orientation with regards to the jet. The "standard model" of AGN's can be seen in Figure 2.1. The observations for radio-loud AGN's are explained in this model as follows: If our field of view is aligned with the jet we observe a blazar (containing both BL Lacs and FSRQs) where the

Radio-loudness	Optical emission line properties		
	Type 2 (narrow lines)	Type 1 (broad lines)	Type 0 (weak/absent)
Radio-quiet	Seyfert 2	Seyfert 1 QSO	
Radio-loud	NLGR (FR I, FR II)	BLGR SSRQ, FSRQ	Blazars (BL Lac, FSRQ)
Decreasing jet angle to line of sight $\rightarrow$			

Table 2.1: A table of the different types of AGN's sorted by their optical emission line properties and their radio-loudness. NLRG and BLRG are narrow and broad line radio galaxies, SSRQ and FSRQ are steep and flat spectrum radio quasars, QSO are quasi-stellar object and FR I and FR II are Fanaroff-Riley Type 1 and 2 radio galaxies. Taken from Ref [17].

jet masks the lines. At larger angles of  $\sim 30^\circ$  one observes a steep-spectrum-radio quasar which is at an angle such that the emission from the accretion disk is observed. A regular radio galaxy (FRI and FRII) is observed at approximately  $90^\circ$ 's to the jet where the torus hides the accretion disk and only narrow lines are observed in the optical spectrum. The same goes for radio-quiet objects all shown in Figure 2.1.



## 3 — Plasmas and Instabilities

This chapter introduces the basic theory of a plasma. We start with its definition and then look at different ways of describing it, namely, the single particle description and a description through its collective behavior using the Vlasov equation. We then introduce the concept of instabilities and look at how this functions in a plasma.

### 3.1 Plasmas

Most matter in the universe is in a state of plasma. This includes stars, the intergalactic medium and the outer layers of our atmosphere. Plasmas are the fourth state of matter, the other three being solids, fluids and gases. The state of a matter is decided by the strength of the bonds between its particles with the bond being strong in solids, weak in fluids and mostly absent in gases. The strength of the bond is determined by the random kinetic energy in the system. If one adds kinetic energy to the system the bonds will weaken and eventually the state will change from solid to fluid or fluid to gas. If enough energy is added a gas will eventually be ionized and possibly become a plasma. A plasma is not equivalent to an ionized gas, but is a state of matter which satisfies certain additional conditions, which we define in the following. Before talking about these criteria we need to define a couple of quantities that describe the plasma.

The plasma has to be macroscopically neutral. The particles constituting the plasma however are charged and interact through the Coulomb potential

$$\phi = \frac{q}{4\pi\epsilon_0 r}. \quad (3.1)$$

The collective effects of the medium causes the charges to arrange themselves in such a way as to cancel out the potential over longer distances. This effects makes the potential exponentially suppressed after a certain distance

$$\phi_D = \frac{q}{4\pi\epsilon_0 r} e^{-r/\lambda_D}, \quad (3.2)$$

where the characteristic distance  $\lambda_D$  is known as the Debye length. It gives the distance at which the thermal kinetic energy equals the electric potential from a charge. The thermal kinetic energy disturbs the medium's electrical neutrality while the electric potential restores it [19]. At distances larger than the Debye length the electric force is suppressed and the thermal kinetic energy dominates. The particle from which the potential originates therefore does not affect particles further away

than the Debye length. An expression for the Debye length can be found by equating the electric potential and the thermal kinetic energy giving [20]

$$\lambda_D = \left( \frac{\epsilon_0 k_B T}{n q^2} \right)^{1/2}. \quad (3.3)$$

This length parameter can be used to define a sphere known as the Debye sphere. It has a volume of  $\frac{4\pi}{3} \lambda_D^3$ . The number of particles inside debye sphere is  $\frac{4\pi}{3} n \lambda_D^3$ . The last factors of this expression is known as the plasma parameter [20]

$$\Lambda = n \lambda_D^3. \quad (3.4)$$

Another important quantity is the plasma frequency. When particles are subjected to an external force displacing them from their equilibrium position collective particle motion arise in the medium trying to restore the medium to its original equilibrium. These motions can be described by a characteristic frequency known as the plasma frequency. An external force will affect the electrons much more than the ions because the electrons are much lighter. The plasma frequency is therefore the frequency of their movement. The expression for the plasma frequency is [20]

$$\omega_p = \left( \frac{n_e e^2}{m_e \epsilon_0} \right)^{1/2}. \quad (3.5)$$

Now we can define the condition required for a material to be a plasma. The first is that  $\lambda_D \ll L$  where  $L$  is the a characteristic dimension of the plasma. That is, the Debye length is much smaller than the scale of the plasma. This is required for the shielding effect (the suppression of electric potential at distances) to be present making the plasma macroscopically neutral. This shielding effect is a result of the collective behaviour in the plasma which requires many charges to be present in a Debye sphere. This leads to the second condition, namely that  $\Lambda \gg 1$ . The third condition is  $\omega_p \tau \gg 1$  where  $\tau$  is the average time between collisions between electrons and neutral particles. The inequality represents the requirement that the frequency of collisions between electrons and neutrals must be much smaller than the plasma frequency. If the collision with neutrals are of the same order as the plasma frequency the plasma will not create oscillations in response to an external force and therefore not act as a plasma.

The simplest way of describing a plasma is through single-particle motion, where the motion of each individual particle can be treated as independent. This is a situation where the charged particles does not directly interact with each other and does not change the external magnetic field in a significant way. Non-relativistic single particles in an electromagnetic-field satisfies the equation of motion

$$m \frac{d\mathbf{v}}{dt} = q(\mathbf{E} + \mathbf{v} \times \mathbf{B}). \quad (3.6)$$

In the absence of an electric field and with a magnetic field in the  $z$ -direction the equation of motion for the components of the velocity becomes

$$\begin{aligned} m\dot{v}_x &= qBv_y \\ m\dot{v}_y &= -qBv_x \\ m\dot{v}_z &= 0. \end{aligned} \quad (3.7)$$

The velocity parallel to the magnetic field is constant. Taking the double derivative results in

$$\begin{aligned}\ddot{v}_x &= -\omega_g^2 v_x \\ \ddot{v}_y &= -\omega_g^2 v_y,\end{aligned}\tag{3.8}$$

with the gyrofrequency

$$\omega_g = \frac{qB}{m}.\tag{3.9}$$

The charged particles gyrate around a guiding centre with this frequency. If we look back at the equation of motion (3.6) we can see that the electric field can be cancelled by giving the whole plasma a drift

$$\mathbf{v}_E = \frac{\mathbf{E} \times \mathbf{B}}{B^2}.\tag{3.10}$$

This is the drift velocity of the guiding center which the charges gyrate around. The drift velocity has many components, such as the polarization drift

$$\mathbf{v}_P = \frac{1}{\omega_{gs} B} \frac{d\mathbf{E}_\perp}{dt}\tag{3.11}$$

for a time varying electric field.

Generally, single-particle motion and effects are hidden in a plasma. The true nature of a plasma is described through its collective behaviour, namely the interaction between particles and fields. The Maxwell equations

$$\text{curl } \mathbf{E} = -\frac{\partial \mathbf{B}}{\partial t}, \quad \text{div } \mathbf{B} = 0,\tag{3.12}$$

$$\text{curl } \mathbf{B} = \mu_0 \mathbf{J} + \frac{1}{c^2} \frac{\partial \mathbf{E}}{\partial t}, \quad \text{div } \mathbf{E} = \frac{\rho}{\epsilon_0}.\tag{3.13}$$

govern this behaviour. The current and charge densities are defined as

$$\begin{aligned}\rho &= \sum_s q_s n_s v_s \\ \mathbf{j} &= \sum_s q_s n_s \mathbf{v}_s,\end{aligned}\tag{3.14}$$

where the sum is over all species of particles. The fundamental equation for collisionless plasma dynamics is the Vlasov equation

$$\left[ \frac{\partial}{\partial t} + \mathbf{v} \cdot \nabla + \frac{q_s}{m_s} (\mathbf{E} + \mathbf{v} \times \mathbf{B}) \cdot \frac{\partial}{\partial \mathbf{v}} \right] f_s(\mathbf{x}, \mathbf{v}, t) = 0.\tag{3.15}$$

which is derived from fluid-dynamics [19]. The function  $f(\mathbf{x}, \mathbf{v}, t)$  is the particle distribution in phase-space. This equation, in addition to the Maxwell equations with the definitions of charge and current density, form a self-consistent set of non-linear equations that is used as the basis for collisionless plasma physics.

Small disturbances can propagate through this system. If the amplitude of these

disturbances is small,  $|\delta A(x, t)| \ll |A_0(x, t)|$ , they can be represented as waves with frequency  $\omega(\mathbf{k})$  and wavenumber  $\mathbf{k}$ . These waves have the phase and group velocity

$$\begin{aligned}\mathbf{v}_p &= \frac{\omega(\mathbf{k})}{k^2} \mathbf{k} \\ \mathbf{v}_g &= \frac{\partial \omega(\mathbf{k})}{\partial \mathbf{k}}.\end{aligned}\tag{3.16}$$

The phase velocity gives the direction of propagation and speed of the wave fronts while the group velocity gives the direction and speed of the energy. The dispersion relation is a connection between the frequency and the wavenumber. In the linear approximation the Vlasov-Maxwell equations is a set of linear equations with the solution

$$D(\omega, \mathbf{k}) = 0.\tag{3.17}$$

This is the dispersion relation of this system. The dispersion relation has the solutions [20]

$$D(\omega, \mathbf{k}) = \text{Det} \left[ \frac{k^2 c^2}{\omega^2} \left( \frac{\mathbf{k}\mathbf{k}}{k^2} - \mathbf{1} \right) + \epsilon(\omega, \mathbf{k}) \right] = 0.\tag{3.18}$$

In this equation  $\epsilon$  is the dielectric tensor. The frequency as a function of the wavenumber,  $\omega = \omega(\mathbf{k})$ , is found using this equation and has many different solutions, each of which describes a different wave mode. Plasmas contain both transverse electromagnetic waves and longitudinal electrostatic waves. This differentiate plasmas from the vacuum which only allows transverse waves. There are many more wave modes in a plasma such as the electrostatic modes which are oscillations of the electrostatic potential and are confined to the plasma. Some of the electromagnetic waves can leave the plasma, namely the O-mode and the high-frequency branch of the X-mode. Other low frequency electromagnetic modes are confined to the plasma. The same is true for the magnetohydrodynamic modes such as the Alfvén-waves, slow and fast mode [20].

Waves in a plasma can experience reflection and resonance. Reflection of a wave occurs when the wavenumber becomes zero while the frequency remains finite. This rotates the wave with an angle of  $\pi$ . Resonance occurs when the wavenumber diverges to infinity. This causes the frequency to become very large which increases the interaction with plasma particles. The wave will then either dissipate its energy to the particles or extract energy to grow. The effects of reflection and resonance is hidden if one only looks at the real part of the solution of the dispersion relation. If one instead looks at solutions on the form

$$\omega = \omega_r(\mathbf{k}) + i\gamma(\omega, \mathbf{k})\tag{3.19}$$

all these plasma effects become apparent.  $\gamma(\omega, \mathbf{k})$  is called the growth rate when  $\gamma$  is negative and the dampening rate when  $\gamma$  is positive. If  $\gamma$  is negative the plasma is unstable. In this thesis the  $\gamma$  factor will be called the absorption coefficient when its sign is not specified.

## 3.2 Plasma Instabilities

In general the stability of a system is determined by how it reacts to a small perturbation. A stable system will dampen and return to its equilibrium while in an

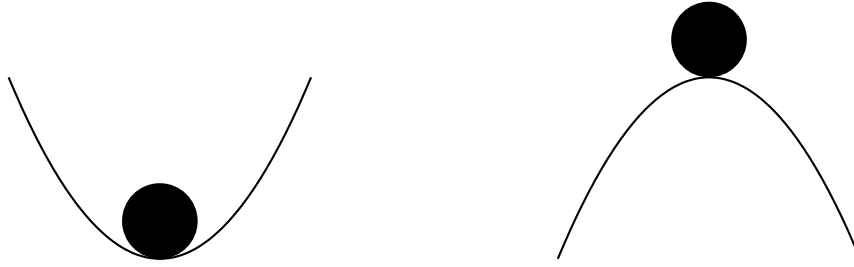


Figure 3.1: An illustration of a stable system (left) and an unstable system (right).

unstable system the perturbation will grow indefinitely. A simple way to visualize this is to think of a ball on the bottom of a valley compared to one atop of a hill as in Figure 3.1. If one pushes the ball at the bottom it will move a short distance up the valley and then fall back and up the other side. After some time the ball will again come to rest at the bottom because of friction. This system is stable. On the other hand, if one pushes the ball at the top of the hill it will roll down gaining more and more speed. The ball will never return to the position at the top of the hill. This system is unstable.

In a plasma the stability of a wave is determined by its interaction with charged particles, i.e. whether it gains or loses energy by this interaction. The stability is represented by the growth rate. The wave amplitude of this interaction is

$$\delta A = \sum_{\mathbf{k}} A_{\mathbf{k}} \exp(-(i\mathbf{k} \cdot \mathbf{x} - i\omega t)). \quad (3.20)$$

The frequency is  $\omega = \omega_r + i\gamma$ . If  $\gamma < 0$  the amplitude grows exponentially and the wave has an unstable growth. Instabilities can be divided into two main categories: Microscopic and macroscopic instabilities. They are macroscopic if the scales are comparable to the bulk size of the plasma and microscopic if the scale are comparable to the gyration radius. Kinetic effects are dominant in microscopic instabilities and therefore they are often known as kinetic instabilities. Macroscopic instabilities are usually more related to fluid theory. Examples of microscopic instabilities are two-stream instability and beam instability. Rayleigh-Taylor and Farley-Buneman instabilities are examples of macroscopic ones [20].



# 4 — Covariant Plasma theory

This thesis utilizes a covariant formalism of plasma theory. In this chapter we first introduce the covariant formalism of special relativity and then use it to find a covariant wavefunction and eventually an expression for the absorption coefficient.

## 4.1 Special Relativity and Covariant Formalism

Special relativity, discovered by Einstein in 1905, is a physical theory of the relationship between time and space. It is based on two postulates. That all physical laws are invariant in all inertial systems and that the speed of light,  $c$ , is the same in all inertial frames. These two assumptions forces one to abandon the idea of absolute time and Galilean transformations and therefore also Newtonian mechanics. Because time is relative and differ in two different inertial systems, it becomes a coordinate. With the space coordinates this describes the four-dimensional spacetime  $(t, x, y, z)$ . The geometry of spacetime is described by the invariant length  $ds^2 = (cdt)^2 - dx^2 - dy^2 - dz^2$ . This spacetime is flat and is often called Minkowski space. The relationship between two reference frames is described by the Lorentz transformations, and relates the coordinates of two inertial frames  $S$  and  $S'$  moving with a relative velocity  $v$  along the  $x$ -axis as

$$\begin{aligned}t' &= \gamma(t - vx/c^2), \\x' &= \gamma(x - vt), \\y' &= y, \\z' &= z,\end{aligned}\tag{4.1}$$

where  $\gamma = (1 - v^2/c^2)^{-1/2}$  is known as the Lorentz factor.

Newtonian mechanics has to be changed in order to incorporate these new ideas. This is done by introducing four-vectors. A four-vector is a line segment in four-dimensional flat spacetime. Four-vectors follow the same rules for addition and multiplication by a scalar as three-vectors. A four-vector is called spacelike if its length in space coordinates are longer than the length in time coordinates and timelike if the length in the time coordinate is longer than the space coordinates. If it is the same length in time and space coordinates it is called lightlike and has zero length. That is, the vector is spacelike if  $ds^2 < 0$ , timelike if  $ds^2 > 0$  and lightlike if  $ds^2 = 0$ .

A general four-vector  $a = (a^0, a^1, a^2, a^3)$  can be written in a basis as  $a = a^0e_0 + a^1e_1 + a^2e_2 + a^3e_3 = \sum_{\alpha=0}^3 a^\alpha e_\alpha$ . Usually the sum is not written explicitly and  $a^\alpha e_\alpha$  is understood to imply the sum over all indicies. This is known as Einsteins

summation convention. Scalar products of four-vectors obey the rules

$$a \cdot b = b \cdot a, \quad (4.2)$$

$$a \cdot (b + c) = a \cdot b + a \cdot c, \quad (4.3)$$

$$(\alpha a) \cdot b = \alpha(a \cdot b). \quad (4.4)$$

where  $a, b, c$  are four-vectors and  $\alpha$  is a scalar. The scalar product of two four-vectors can be calculated using their basis

$$a \cdot b = (a^\alpha e_\alpha) \cdot (b^\beta e_\beta) = (e_\alpha \cdot e_\beta) a^\alpha b^\beta. \quad (4.5)$$

The tensor product defines a rank-2 tensor  $\eta_{\alpha\beta} = e_\alpha \cdot e_\beta$  known as the metric tensor. With this the scalar product is

$$a \cdot b = \eta_{\alpha\beta} a^\alpha b^\beta, \quad (4.6)$$

and can be calculated if one knows the metric tensor. In Minkowski space the metric tensor is

$$\eta_{\alpha\beta} = \begin{pmatrix} 1 & 0 & 0 & 0 \\ 0 & -1 & 0 & 0 \\ 0 & 0 & -1 & 0 \\ 0 & 0 & 0 & -1 \end{pmatrix}, \quad (4.7)$$

which means that the scalar product of two four vectors in Minkowski space is  $a \cdot b = a^0 b^0 - a^1 b^1 - a^2 b^2 - a^3 b^3 = a^0 b^0 - \mathbf{a} \cdot \mathbf{b}$ . If the index on a four-vector is down it is a covariant vector while it is called a contravariant vector if the index is up. Covariant and contravariant vectors are connected by the metric tensor  $x^\mu = \eta^{\mu\nu} x_\nu$ . The invariant length  $ds$  can be written  $ds^2 = dx^\mu dx_\mu$ .

With these new vectors one can create relativistic mechanics. This is a covariant formalism of Newtonian mechanics containing the same equations, but with four-vectors in Minkowski space as opposed to three-vectors in Euclidean space.

## 4.2 Covariant Plasma Theory

From here on out we will be using natural units with  $c = \hbar = k_B = 1$  unless otherwise stated. The electromagnetic field is described by the electric field strength  $\mathbf{E}$  and the magnetic induction  $\mathbf{B}$  in addition to the charge density  $\rho$  and the current density  $\mathbf{J}$ . These quantities are related by Maxwell's equations (3.12) and (3.13) which can be written in covariant form as

$$\partial^\mu F^{\nu\rho}(x) + \partial^\rho F^{\mu\nu}(x) + \partial^\nu F^{\rho\mu}(x) = 0, \quad (4.8)$$

$$\partial_\mu F^{\mu\nu}(x) = \mu_0 J^\nu(x), \quad (4.9)$$

where  $F^{\mu\nu}(x)$  is the Maxwell tensor

$$F^{\mu\nu}(x) = \begin{pmatrix} 0 & -E^1/c & -E^2/c & -E^3/c \\ E^1/c & 0 & -B^3 & B^2 \\ E^2/c & B^3 & 0 & -B^1 \\ E^3/c & -B^2 & B^1 & 0 \end{pmatrix}. \quad (4.10)$$



We now introduce the vector field  $A^\mu = (\phi, \mathbf{A})$  where  $\phi$  and  $\mathbf{A}$  are connected to the electric field strength and magnetic induction by  $\mathbf{B} = \nabla \times \mathbf{A}$  and  $\mathbf{E} = -\nabla\phi - \partial\mathbf{A}/\partial t$ . In terms of this vector field  $A^\mu(x)$  the Maxwell tensor can be expressed as

$$F^{\mu\nu}(x) = \partial^\mu A^\nu(x) - \partial^\nu A^\mu(x). \quad (4.11)$$

The wave equation is obtained by Fourier transforming equation (4.9)

$$\begin{aligned} k_\mu F^{\mu\nu}(k) &= \mu_0 J^\nu(k) \\ k_\mu(k^\mu A^\nu(k) - k^\nu A^\mu(k)) &= \mu_0 J^\nu(k) \\ (k^2 \eta^{\mu\nu} - k^\mu k^\nu) A_\nu(k) &= \mu_0 J^\nu(k). \end{aligned} \quad (4.12)$$

The current  $J^\mu(k)$  can be separated into an induced part that describes the response of a medium and an extraneous part which is a source term

$$J^\mu(k) = J_{\text{ind}}^\mu(k) + J_{\text{ext}}^\mu(k). \quad (4.13)$$

The linear response can be defined by the induced current as

$$J_{\text{ind}}^\mu(k) = \Pi^\mu{}_\nu(k) A^\nu(k). \quad (4.14)$$

$\Pi^\mu{}_\nu(k)$  is the linear response tensor and will be discussed in chapter 5. Using this the wave equation (4.12) can be rewritten as

$$\begin{aligned} (k^2 \eta^{\mu\nu} - k^\mu k^\nu + \mu_0 \Pi^{\mu\nu}(k)) A_\nu(k) &= -\mu_0 J_{\text{ext}}^\mu(k) \\ \Lambda^{\mu\nu}(k) A_\nu(k) &= -\mu_0 J_{\text{ext}}^\mu(k). \end{aligned} \quad (4.15)$$

with  $\Lambda^{\mu\nu}$  defined as  $\Lambda^{\mu\nu} \equiv k^2 \eta^{\mu\nu} - k^\mu k^\nu + \mu_0 \Pi^{\mu\nu}(k)$ . We want to solve the wave equation (4.12). To do this we introduce the photon propagator  $D^{\mu\nu}(k)$ . The photon propagator is a Green's function defined as the solution of

$$\Lambda^\mu{}_\nu(k) D^{\nu\rho}(k) = \mu_0 \eta^{\mu\rho}. \quad (4.16)$$

Using the charge-continuity relation  $kJ(k) = 0$  this equation can be rewritten as

$$\Lambda^\mu{}_\nu(k) D^{\nu\rho}(k) = \mu_0 (\eta^{\mu\rho} - k^\mu k^\rho / k^2) \quad (4.17)$$

which serves as a convenient definition of  $D^{\mu\nu}(k)$ . A problem in deriving the propagator comes from the fact that the determinant of  $\Lambda^{\mu\nu}$  is zero. This can be shown by first noting that the charge-continuity equation implies  $k_\mu \Lambda^{\mu\nu}(k) = 0$  (as can be seen by contracting the wave equation (4.12) with  $k_\mu$ ). This implies that  $k_\mu$  is an eigenvector of  $\Lambda^{\mu\nu}$  with eigenvalue 0, thusly  $\Lambda^{\mu\nu}$  has a determinant of 0. This means that  $\Lambda^{\mu\nu}$  has no inverse. It also means that its matrix of cofactors  $\lambda^{\mu\nu}$  is of rank one. Being a rank one matrix it can be written as the outer product of a vector with itself. Since  $k_\mu$  is an eigenvector of  $\Lambda^{\mu\nu}$  it can be used to express

$$\lambda^{\mu\nu}(k) = \lambda(k) k^\mu k^\nu \quad (4.18)$$

which is the matrix of cofactors with the invariant  $\lambda(k)$ . A solution to equation (4.17) is found by using the second order matrix of cofactors  $\lambda^{\mu\alpha\nu\beta}$ . The second order matrix of cofactors satisfies

$$\Lambda^\mu{}_\rho(k) \lambda^{\rho\nu\alpha\beta}(k) = \lambda(k) [\eta^{\mu\alpha} k^\nu k^\beta - \eta^{\mu\beta} k^\nu k^\alpha]. \quad (4.19)$$

In order to find an expression for the photon propagator we contract the equation with  $k_\nu k_\beta$

$$\begin{aligned} k_\nu k_\beta \Lambda^\mu{}_\rho(k) \lambda^{\rho\nu\alpha\beta}(k) &= \lambda(k) [k_\nu k_\beta \eta^{\mu\alpha} k^\nu k^\beta - k_\nu k_\beta \eta^{\mu\beta} k^\nu k^\alpha] \\ &= \lambda(k) k^4 \left[ \eta^{\mu\nu} - \frac{k^\mu k^\alpha}{k^2} \right], \end{aligned} \quad (4.20)$$

and rewrite it as

$$\Lambda^\mu{}_\rho \mu_0 \frac{\lambda^{\rho\nu\alpha\beta} k_\nu k_\beta}{\lambda(k) k^4} = \mu_0 \left[ \eta^{\mu\nu} - \frac{k^\mu k^\alpha}{k^2} \right]. \quad (4.21)$$

Now, comparing this with equation (4.17) the photon propagator is

$$D^{\mu\nu}(k) = \mu_0 \frac{k_\alpha k_\beta \lambda^{\mu\alpha\nu\beta}(k)}{k^4 \lambda(k)}. \quad (4.22)$$

This is a specific solution to equation (4.17). If we want a general solution we can modify the photon propagator  $D'^{\mu\nu} = D^{\mu\nu} + \xi^\mu(k) k^\nu + \zeta^\nu(k) k^\mu$  with the  $\xi(k)$  and  $\zeta(k)$  are arbitrary.

### 4.3 Wave Energetics and the Absorption Coefficient

In order to find an expression for the absorption coefficient we need to find the rate of momentum transfer from an extraneous current to the wave field and the wave energy. We will see that mathematically the absorption coefficient is described by the dissipative, anti-hermitian, part of the LRT.

Firstly, the hermitian and anti-hermitian part of a tensor is defined as

$$\begin{aligned} \Pi^{H\mu\nu}(k) &= \frac{1}{2} [\Pi^{\mu\nu}(k) + \Pi^{*\mu\nu}(k)] \\ \Pi^{A\mu\nu}(k) &= \frac{1}{2} [\Pi^{\mu\nu}(k) - \Pi^{*\mu\nu}(k)]. \end{aligned} \quad (4.23)$$

It should be noted that for a symmetric tensor the hermitian part of the tensor is equal to its real part and the anti-hermitian part is equal to its imaginary part.

We use a rather unintuitive way of finding the wave energy. First we find the ratio of electric to total energy and then we find the total energy. The electric energy, which is the same as the wave energy, is then the ratio of these two factors. From Ref [14] the ratio of electric to total energy is

$$R_M(k) = \frac{\lambda^{0\sigma}{}_{0\sigma}(k)}{\omega \partial \lambda(k) / \partial \omega} \Big|_{k=k_M}, \quad (4.24)$$

which can be rewritten as

$$[R_M(k)]^{-1} = - \left[ \frac{1}{\omega} \frac{\partial}{\partial \omega} \Lambda_M(k) \right] \Big|_{\omega=\omega_M}, \quad (4.25)$$

with  $\Lambda_M(k) = e_{M\mu}^*(k)e_{M\mu}(k)\Lambda^{H\mu\nu}(k)$ .  $R_M$  is connected to the wave function renormalization constant  $Z$  as  $R_M^{1/2} \propto Z^{1/2}$ .

The wave amplitude  $a_M(k)$  for a mode  $M$  is defined by the four-potential

$$A_M^\mu(x) = V \int \frac{d^4k}{(2\pi)^4} a_M(k) e_M^\mu(k) e^{-ikx} 2\pi \delta[\omega - \omega_M(\mathbf{k})]. \quad (4.26)$$

The inclusion of a volume  $V$  gives  $A_M^\mu(x)$  and  $a_M(k)$  the same dimensions. After a Fourier transformation, equation (4.26) becomes

$$A_M^\mu(k) = V a_M(k) e_M^\mu(k) 2\pi \delta[\omega - \omega_M(\mathbf{k})]. \quad (4.27)$$

The electric energy density in waves for an electric field is  $\frac{1}{2}\epsilon_0|\mathbf{E}|^2$ . The total electric energy density is obtained by averaging this over all time and space by integrating and normalizing with a factor  $1/TV$ . In the temporal gauge one has

$$\frac{1}{TV} \int d^4x \frac{1}{2} \epsilon_0 |\mathbf{E}(x)|^2 = \frac{1}{TV} \int \frac{d^4k}{(2\pi)^4} \frac{1}{2} \epsilon_0 |\omega \mathbf{A}(k)|^2. \quad (4.28)$$

For a wave in mode  $M$  the average energy is

$$\begin{aligned} \frac{1}{TV} \int \frac{d^4k}{(2\pi)^4} \frac{1}{2} \epsilon_0 |\omega \mathbf{A}_M(k)|^2 &= \frac{1}{TV} \int \frac{d^4k}{(2\pi)^4} \epsilon_0 |\omega V a_M(k)|^2 |\mathbf{e}_M(k)|^2 |2\pi \delta[\omega - \omega_M(\mathbf{k})]|^2 \\ &= V \int \frac{d^4k}{(2\pi)^4} \epsilon_0 |\omega a_M(k)|^2 2\pi \delta[\omega - \omega_M(\mathbf{k})] = V \epsilon_0 \int \frac{d^3\mathbf{k}}{(2\pi)^3} |\omega_M a_M(k)|^2, \end{aligned} \quad (4.29)$$

where we have rewritten the square of the delta function as  $[2\pi\delta(\omega - \omega_M(\mathbf{k}))]^2 = T2\pi\delta(\omega - \omega_M(\mathbf{k}))$  and gained a factor 2 by including the contribution of both the positive and the negative frequency solutions. The last integral is still the average over the electric energy which makes the integrand, with the factor  $V\epsilon_0$ , the electric energy of waves in mode  $M$ . Let the total energy of the waves in mode  $M$  be denoted by  $W_M$ .  $W_M$  is given by

$$W_M(k) = \frac{\epsilon_0 V |\omega_M(k) a_M(k)|^2}{R_M(k)}, \quad (4.30)$$

that is the electric energy divided by the ratio of electric to total energy. One wishes to normalize to one wave quantum with energy  $W_M(k) = \omega_M(k)$ . This gives the normalization condition

$$a_M(k) = \left( \frac{R_M(k)}{V \epsilon_0 \omega_M(k)} \right)^{1/2}. \quad (4.31)$$

Next we find the rate  $Q_M^\mu$  of momentum transfer from an extraneous current to the wave field. The four-momentum is generated by a current  $J^\alpha(x)$  at a rate  $J_\alpha F^{\alpha\mu}$ . The average rate of momentum transfer by an extraneous current is given by integrating the rate over spacetime normalized by  $1/T$ . A Fourier transformation into  $k$ -space results in

$$\frac{1}{T} \int d^4x J_{\text{ext}}^\alpha(x) F_\alpha^\mu(x) = -\frac{i}{T} \int \frac{d^4k}{(2\pi)^4} k^\mu J_{\text{ext}}^\alpha(k) A_\alpha(k). \quad (4.32)$$

The extraneous current is related to the dissipative, anti-hermitian, part of the LRT as  $J^\alpha(k) = \Pi^{A\alpha\beta}(k)A_\beta(k)$ . With this relation the equation (4.32) can be rewritten as follows

$$\begin{aligned}
& -\frac{i}{T} \int \frac{d^4k}{(2\pi)^4} k^\mu A_\alpha(k) \Pi^{A\alpha\beta}(k) A_\beta(k) \\
&= -\frac{i}{T} V^2 \int \frac{d^4k}{(2\pi)^4} k^\mu |a(k)|^2 [2\pi\delta(\omega - \omega_M(\mathbf{k}))]^2 e_{M\alpha}^*(k) \Pi^{A\alpha\beta} e_{M\beta}(k) \\
&= iV^2 \int \frac{d^4k}{(2\pi)^4} k^\mu \frac{R_M(k)}{V\epsilon_0\omega_M} 2\pi\delta(\omega - \omega_M(\mathbf{k})) \Pi^A(k) \\
&= -2iV \int \frac{d^3\mathbf{k}}{(2\pi)^3} k_M^\mu \frac{R_M(k)}{\epsilon_0\omega_M} \Pi_M^A.
\end{aligned} \tag{4.33}$$

In the third equality we have employed the normalization condition (4.31). From the last equation the rate of momentum transfer is seen to be

$$Q_M^\mu(k) = -2i \frac{R_M(k)}{\epsilon_0\omega_M(k)} k_M^\mu \Pi_M^A(k_M). \tag{4.34}$$

Armed with both the rate of momentum transfer and the wave energy we can find the absorption coefficient. The 0-component of the rate of momentum transfer is the rate of energy transfer. The rate of energy transfer to the wave field from an extraneous current is proportional to the wave energy by a factor  $\gamma_M$

$$Q_M^0(k) = -\gamma_M(k)W_M(k). \tag{4.35}$$

This proportionality factor is the absorption coefficient. The wave energy varies exponentially with this factor as can be seen by rewriting equation (4.35), using that the rate of energy transfer is the derivative of the wave energy,

$$\frac{\partial W_M(k)}{\partial t} = -\gamma_M(k)W_M(k). \tag{4.36}$$

The solution of this differential equation is simply

$$W_M(k) = C e^{-\gamma_M(k)t}. \tag{4.37}$$

Finally we find the explicit expression for the absorption coefficient, which is

$$\gamma_M(k) = -\frac{Q_M^0(k)}{W_M(k)} = 2i \frac{R_M(k)}{\epsilon_0\omega_M(k)} \Pi_M^A(k_M). \tag{4.38}$$

# 5 — The Linear Response Tensor

The linear response tensor is needed to find the absorption coefficient in this theory. In this chapter the LRT for a plasma with momentum distribution strictly parallel to the direction of propagation travelling through a background plasma is calculated. Firstly the weak-turbulence expansion, the expansion of an induced current in the amplitude of the electromagnetic (EM) field, is introduced. Then the Lagrangian, and the subsequent equation of motion (EoM), for a collection of charged particles in an EM field is derived. With this EoM we use the forward-scattering method to find the current for a single particle and then the LRT by comparing the current to the weak-turbulence expansion.

## 5.1 The Weak-Turbulence Expansion

The wave equation in  $k$ -space is

$$[k^2 g^{\mu\nu} - k^\mu k^\nu] A_\nu(k) = -\mu_0 J^\mu(k), \quad (5.1)$$

where the current can be split into an induced and extraneous part

$$J^\mu(k) = J_{\text{ind}}^\mu(k) + J_{\text{ext}}^\mu(k). \quad (5.2)$$

The induced current describes the response of the medium and the extraneous part acts as a source term. If the induced current is assumed to be weak it can be expanded in terms of the amplitude of the EM field,  $A^\mu(k)$ , which converges rapidly. This is the weak-turbulence expansion [14],

$$\begin{aligned} J_{\text{ind}}^\mu(k) &= \Pi^\mu{}_\nu(k) A^\nu(k) + \int d\lambda^{(2)} \Pi^{(2)\mu}{}_{\nu\rho}(-k, k_1, k_2) A^\nu(k_1) A^\rho(k_2) \\ &+ \int d\lambda^{(3)} \Pi^{(3)\mu}{}_{\nu\rho\sigma}(-k, k_1, k_2, k_3) A^\nu(k_1) A^\rho(k_2) A^\sigma(k_3) + \dots \\ &+ \int d\lambda^{(n)} \Pi^{(n)\mu}{}_{\nu_1\nu_2\dots\nu_n}(-k, k_1, k_2, \dots, k_n) A^{\nu_1}(k_1) A^{\nu_2}(k_2) \dots A^{\nu_n}(k_n) \\ &+ \dots, \end{aligned} \quad (5.3)$$

where  $d\lambda^{(n)}$  is defined as

$$d\lambda^{(n)} = \frac{d^4 k_1}{(2\pi)^4} \frac{d^4 k_2}{(2\pi)^4} \dots \frac{d^4 k_n}{(2\pi)^4} (2\pi)^4 \delta^4(k - k_1 - k_2 - \dots - k_n). \quad (5.4)$$

This expansion defines the LRT,  $\Pi^{\mu\nu}(k)$ , which describes the medium's linear response.

## 5.2 Lagrangian Density

The action integral can be used to find the EoM for a system. For a system consisting of free particles and an EM field the action integral can be expressed by the Lagrangian density,  $\mathcal{L}$ , as [14]

$$I = \int d^4x \mathcal{L}(x), \quad \mathcal{L} = \sum \mathcal{L}_P(x) + \mathcal{L}_{EM}(x). \quad (5.5)$$

The Lagrangian has the term  $\sum \mathcal{L}_P(x)$  describing the free particles, with the sum being all species of particles, and  $\mathcal{L}_{EM}(x)$  describing the free EM field. The non-covariant Lagrangian for a single particle, with charge  $q$  and mass  $m$ , is

$$L(\mathbf{x}, \mathbf{v}, t) = -m(1 - \mathbf{v}^2)^{1/2} - q\phi(t, \mathbf{x}) + q\mathbf{v} \cdot \mathbf{A}(t, \mathbf{x}), \quad (5.6)$$

where  $\phi(t, \mathbf{x})$  and  $\mathbf{A}(t, \mathbf{x})$  are the scalar and vector potential for the EM field. Using the proper time,  $\tau$ , the covariant Lagrangian is defined by writing the action integral as

$$I = \int d\tau R(x, u), \quad R(x, u) = -m - quA(x), \quad (5.7)$$

where  $\tau = dt/\gamma$  and  $R(x, u) = \gamma L(\mathbf{x}, \mathbf{v}, t)$ .

The EoM can be found by using the action principle,  $\delta I = 0$ . That is

$$0 = \delta I = \int d\tau \left[ \frac{d\delta\tau}{d\tau} + \delta x^\mu \partial_\mu + \delta u^\mu \frac{\partial}{\partial u^\mu} \right] R(x, u). \quad (5.8)$$

Rewriting the action integral equation (5.8) leads to a covariant EoM

$$\frac{d}{d\tau} \left\{ \left[ (g^{\mu\nu} - u^\mu u^\nu) \frac{\partial}{\partial u^\mu} + u^\mu \right] R(x, u) \right\} - \partial^\mu R(x, u) = 0. \quad (5.9)$$

A simpler way to find to covariant EoM is to start with a covariant form of Newton's equation

$$\frac{dp^\mu}{d\tau} = \mathcal{F}^\mu. \quad (5.10)$$

When the EM force is the the only one acting on the particle the force is the Lorentz force  $\mathcal{F} = qF^{\mu\nu}u_\nu$ . After a Fourier transformation to  $k$ -space the EoM becomes

$$\frac{du^\mu(\tau)}{d\tau} = \frac{q}{m} F_0^{\mu\nu} u_\nu(\tau) + \frac{iq}{m} \int \frac{d^4k'}{(2\pi)^4} e^{-ik'x(\tau)} k' u(\tau) G^{\mu\nu}(k', u(\tau)) A_\nu(k'), \quad (5.11)$$

$$G^{\mu\nu}(k, u) = g^{\mu\nu} - \frac{k^\mu u^\nu}{ku}. \quad (5.12)$$

The EM field  $F^{\mu\nu}(k)$  consists of a static field  $F_0^{\mu\nu}(k)$  and a fluctuating field represented by  $A^\mu(k)$ . In this thesis the static field is set to zero.

## 5.3 Forward-Scattering Method

In the the forward-scattering approach all wave are the same before and after scattering. Because of this all the particles in the medium contributes in phase to

forward scattering and the sum of all these contributions corresponds to the collective response of the medium [14]. In this section we want to expand the current in orders of the EM field,  $A(k)$ , and compare the expression to the weak-turbulence expansion in order to identify the LRT.

We now look to expand the current due to a single particle in powers of the potential  $A(k)$ . The motion of the particle is rectilinear in the absence of a static field and its orbit can be represented by

$$X^\mu(\tau) = x_0^\mu + u_0^\mu \tau + \sum_{n=1}^{\infty} X^{(n)\mu}(\tau) = X_0^\mu(\tau) + \sum_{n=1}^{\infty} X^{(n)\mu}(\tau) \quad (5.13)$$

where  $x_0$  and  $u_0$  is constants and  $X^{(n)}(\tau)$  is of  $n$ th order in  $A(k)$ . Similarly the velocity can be expanded

$$u^\mu(\tau) = u_0^\mu + \sum_{n=1}^{\infty} u^{(n)\mu}(\tau). \quad (5.14)$$

The current for a single particle in an orbit  $X^\mu(\tau)$  in  $k$ -space is

$$J_{\text{sp}}^\mu(k) = q \int d\tau u^\mu(\tau) e^{ikX(\tau)} \quad (5.15)$$

and can be expanded in orders of  $A(k)$  by inserting the expansions of the orbit and velocity

$$J_{\text{sp}}^\mu(k) = q \int d\tau \left( u^{(0)\mu} + \sum_{n=1}^{\infty} u^{(n)\mu}(\tau) \right) e^{ikX^{(0)}(\tau)} e^{\sum_{n=1}^{\infty} ikX^{(n)}(\tau)}. \quad (5.16)$$

The expansion to second order is

$$J_{\text{sp}}^{(0)\mu}(k) = q \int d\tau u^{(0)\mu}(\tau) e^{ikX^{(0)}(\tau)}, \quad (5.17)$$

$$J_{\text{sp}}^{(1)\mu}(k) = q \int d\tau \left( u^{(1)\mu}(\tau) + ikX^{(1)}(\tau) u^{(0)\mu}(\tau) \right) e^{ikX^{(0)}(\tau)}, \quad (5.18)$$

$$J_{\text{sp}}^{(2)\mu}(k) = q \int d\tau \left[ u^{(2)\mu}(\tau) + ikX^{(1)}(\tau) u^{(1)\mu}(\tau) + \left( -\frac{1}{2} (kX^{(1)}(\tau))^2 + ikX^{(2)}(\tau) \right) u^{(0)\mu} \right] e^{ikX^{(0)}(\tau)}. \quad (5.19)$$

The EoM (5.11) can also be expanded in terms of  $A(x)$

$$\begin{aligned} \frac{du^\mu(\tau)}{d\tau} &= \frac{iq}{m} \int \frac{d^4k}{(2\pi)^4} e^{-ikX^{(0)}(\tau)} e^{-ikX^{(n)}(\tau)} k' \left( u^{(0)\mu} \tau + \sum_{n=1}^{\infty} u^{(n)\mu}(\tau) \right) \\ &\times G^{\mu\nu} \left( k', u^{(0)\mu} + \sum_{n=1}^{\infty} u^{(n)\mu}(\tau) \right) A_\nu(k'). \end{aligned} \quad (5.20)$$

The terms to second order are

$$\frac{d}{d\tau} u^{(0)\mu}(\tau) = 0, \quad (5.21)$$

$$\frac{d}{d\tau} u^{(1)\mu}(\tau) = \frac{iq}{m} \int \frac{d^4 k'}{(2\pi)^4} e^{-ik'X^{(0)}(\tau)} k' G^{\mu\nu}(k', u^{(0)}) A_\nu(k'), \quad (5.22)$$

$$\begin{aligned} \frac{d}{d\tau} u^{(2)\mu}(\tau) &= \frac{iq}{m} \int \frac{d^4 k'}{(2\pi)^4} e^{-ik'X^{(0)}(\tau)} \left( -ikX^{(1)}(\tau) + u^{(1)}(\tau) \frac{\partial}{\partial u^{(0)}} \right) \\ &\times k' u^{(0)} G^{\mu\nu}(k', u^{(0)}) A_\nu(k). \end{aligned} \quad (5.23)$$

The expanded EoM can be integrated once and twice to find the  $n$ th order velocity and orbit respectively. The current expansion for a single particle then becomes, ignoring the 0 superscript in  $u^{(0)}$ ,

$$\begin{aligned} J_{sp}^{(n)\mu} &= \int \frac{d^4 k_1}{(2\pi)^4} \cdots \int \frac{d^4 k_n}{(2\pi)^4} \beta^{(n)\mu\nu_1 \cdots \nu_n}(k, k_1, \cdots, k_n, u) \\ &\times A_{\nu_1}(k_1) \cdots A_{\nu_n}(k_n) e^{i(k-k_1-\cdots-k_n)x_0} 2\pi \delta[(k-k_1-\cdots-k_n)u] \end{aligned} \quad (5.24)$$

after inserting the velocity and orbit. The first terms of the  $\beta^{(n)\mu\nu_1 \cdots \nu_n}$  are

$$\beta^{(0)\mu}(k, u) = qu^\mu, \quad (5.25)$$

$$\beta^{(1)\mu\nu}(k, k_1, u) = -\frac{q^2}{m} a^{\mu\nu}(k, k_1, u), \quad (5.26)$$

$$\begin{aligned} \beta^{(2)\mu\nu\rho}(k, k_1, k_2, u) &= -\frac{q^3}{2m^2} \left[ a^{\mu\nu}(k, k_1, u) \frac{(k-k_1)_\alpha G^{\alpha\rho}(k_2, u)}{k_2 u} \right. \\ &\left. + a^{\mu\rho}(k, k_2, u) \frac{(k-k_2)_\alpha G^{\alpha\nu}(k_1, u)}{k_1 u} + a^{\nu\rho}(k_1, k_2, u) \frac{(k_1+k_2)_\alpha G^{\alpha\rho}(k, u)}{ku} \right], \end{aligned} \quad (5.27)$$

with

$$a^{\mu\nu}(k, k_1, u) = g^{\mu\nu} - \frac{k^\nu u^\mu}{ku} - \frac{k_1^\nu}{k_1 u} + \frac{kk_1 u^\mu u^\nu}{ku k_1 u} \quad (5.28)$$

and

$$G^{\mu\nu}(k, u) = g^{\mu\nu} - \frac{k^\mu u^\nu}{ku}. \quad (5.29)$$

$J_{sp}^{(n)\mu}$  is the current for a single particle. In order to get the total current from all particles the  $J_{sp}^{(n)\mu}$  is operated on with  $\int [d^4 x_0 d^4 p_0 / (2\pi)^4] F(p_0)$  [14]. This is a statistical average over the initial, unperturbed, position and velocity.  $F(p)$  is the covariant particle distribution function. The covariant and the non-covariant particle distribution functions are related by

$$\frac{d^4 p}{(2\pi)^4} F(p) = \frac{d^3 \mathbf{p}}{(2\pi)^3 \gamma} f(\mathbf{p}) \quad (5.30)$$

and defines the number density and proper number density

$$n(x) = \int \frac{d^4 p}{(2\pi)^4} \gamma F(x, p), \quad n_{pr}(x) = \int \frac{d^4 p}{(2\pi)^4} F(x, p). \quad (5.31)$$

The number density is frame dependent while the proper number density is a constant. However, the proper number density does not correspond to the number density in any frame. The integral over  $x_0$  is just a delta function

$$\int d^4 x_0 e^{i(k-k_1-\cdots-k_n)x_0} = (2\pi)^4 \delta^4(k-k_1-\cdots-k_n). \quad (5.32)$$



This equation shows that only the forward waves contributes to scattering which is the forward-scattering condition. It also indicates translational invariance as the response tensor is independent of the initial position  $x_0$ . Comparing now the total current with the weak-turbulence expansion (5.3) the  $n$ th order response of the medium is

$$\Pi^{(n)\mu\nu_1\dots\nu_n}(-k, k_1, \dots, k_n) = \int \frac{d^4p}{(2\pi)^4} F(p) \beta^{(n)\mu\nu_1\dots\nu_n}(k, k_1, \dots, k_n, n). \quad (5.33)$$

The linear response,  $n = 1$ , is then

$$\Pi^{\mu\nu}(k) = -\frac{q^2}{m} \int \frac{d^4p}{(2\pi)^4} F(p) a^{\mu\nu}(k, u). \quad (5.34)$$

## 5.4 Jüttner Distribution

The Jüttner distribution is a relativistic thermal distribution of particles that acts as the relativistic counterpart to the non-relativistic Maxwellian distribution for particles with a temperature  $T$  and energy  $\epsilon = \gamma m$ . The distribution describes an approximate ideal gas where the particles do not strongly interact. In 6-dimensional phase space the Jüttner distribution is [14]

$$f(\mathbf{p}) = \frac{2\pi^2 n \rho e^{-\rho\gamma}}{m^3 K_2(\rho)}, \quad (5.35)$$

where  $\rho = m/T$  and  $\gamma = (1 - \beta^2)^{-1/2}$  is the Lorentz factor for a velocity  $\beta$ .  $K_2(\rho)$  is a modified Bessel function of the second kind or as we will call it here a MacDonald function. They are defined and discussed thoroughly in appendix A. For a plasma of electrons with  $m \approx 0.550$  MeV  $\rho = 1$  corresponds to a temperature of  $T \approx 5 \cdot 10^9$  K. Thus, for  $\rho = 1$  the plasma is borderline relativistic. It follows that the ultrarelativistic limit is  $\rho \ll 1$  and the nonrelativistic limit is  $\rho \gg 1$ .

For an 8-dimensional phase space in an arbitrary frame, where  $\tilde{u}$  is the velocity in the rest frame, the Jüttner distribution is

$$F(p) = \frac{(2\pi)^3 n \rho}{m^2 K_2(\rho)} \delta(p^2 - m^2) e^{-\rho(p\tilde{u}/m)}. \quad (5.36)$$

## 5.5 The Relativistic Plasma Dispersion Function

In this thesis the relativistic plasma dispersion function (RPDF) is defined to be [14]

$$T(z, \rho) = \int_{-1}^1 d\beta \frac{e^{-\rho\gamma}}{\beta - z}, \quad (5.37)$$

where  $z = \omega/|\mathbf{k}|$  is the phase velocity. The relativistic plasma dispersion function can be rewritten as [14]

$$T(z, \rho) = \begin{cases} -\frac{2\rho}{1-z^2} \int_0^z d\zeta \frac{K_1(\rho R)}{R} + i\pi e^{-\rho\gamma_0} & \text{for } z < 1 \\ \frac{2\rho}{1-z^2} \int_z^\infty d\zeta \frac{K_1(\rho R)}{R} & \text{for } z > 1 \end{cases} \quad (5.38)$$

with  $R = [(1 - \zeta^2)/(1 - z^2)]^{1/2}$  and  $\gamma_0 = (1 - z^2)^{-1/2}$ . This function and some of its derivatives will be useful in the following equations. For the expressions of these derivatives the reader is referred to appendix B. Note that  $T(z, \rho)$  only has an imaginary part for  $z < 1$ . This is because  $-1 < \beta < 1$  and  $T(z, \rho)$  only has a pole for  $z < 1$ . The absorption coefficient which is proportional to the imaginary part is therefore zero for  $z > 1$  (if the phase velocity is larger than the speed of light).

$T(z, \rho)$  can be expanded for ultrarelativistic speeds [14],  $\rho \ll 1$ ,

$$T(z, \rho) = -\ln \left| \frac{1+z}{1-z} \right| + i\pi H(1-z)e^{-\rho\gamma_0} \quad (5.39)$$

with the step function  $H(x)$ . The exponential in the imaginary part should be set to zero in order to consistently only include the leading term in  $\rho$ .

## 5.6 Instability Due to an Anisotropic Strictly-Parallel Thermal Distribution

An anisotropic distribution of particles leads to plasma instabilities [14]. This can be caused by a temperature anisotropy. The thermal distribution is here strictly parallel to a 4-vector,  $b^\mu = [0, \mathbf{b}]$  in the rest frame. With this assumption  $p_\perp$  can be set to zero and the particle distribution function can be written as  $f(\mathbf{p}) = (2\pi)^3 \delta^2(\mathbf{p}_\perp) g(\gamma)$ , where  $g(\gamma)$  is decided by the particle distribution function, in this case the Jüttner distribution. We will now solve the integral in the linear response (5.34) for this distribution.

The response tensor in the forward-scattering method (5.34) can be rewritten as

$$\begin{aligned} \Pi^{\mu\nu}(k) &= -\frac{q^2}{m} \int \frac{d^4p}{(2\pi)^4} F(p) \left[ g^{\mu\nu} - \frac{k^\mu u^\nu + k^\nu u^\mu}{ku} + \frac{k^2 u^\mu u^\nu}{(ku)^2} \right] \\ &= -\frac{q^2}{m} \left[ g^{\mu\nu} \int \frac{d^4p}{(2\pi)^4} F(p) - \frac{k^\mu k^\nu \int \frac{d^4p}{(2\pi)^4} F(p) \frac{u^\nu}{ku} + k^\nu k^\mu \int \frac{d^4p}{(2\pi)^4} F(p) \frac{u^\mu}{ku}}{k\tilde{u}} \right. \\ &\quad \left. + \frac{k^2 (k\tilde{u})^2 \int \frac{d^4p}{(2\pi)^4} F(p) \frac{u^\mu u^\nu}{(ku)^2}}{(k\tilde{u})^2} \right]. \end{aligned} \quad (5.40)$$

Let us now define

$$\begin{aligned} f_1^\mu &= k\tilde{u} \int \frac{d^4p}{(2\pi)^4} F(p) \frac{u^\mu}{ku}, \\ f_2^{\mu\nu} &= (k\tilde{u})^2 \int \frac{d^4p}{(2\pi)^4} F(p) \frac{u^\mu u^\nu}{(ku)^2}, \end{aligned} \quad (5.41)$$

and use (5.31) to write (5.40) as

$$\Pi^{\mu\nu}(k) = -\frac{q^2}{m} \left[ n_{pr} g^{\mu\nu} - \frac{k^\mu f_1^\nu + k^\nu f_1^\mu}{k\tilde{u}} + \frac{k^2 f_2^{\mu\nu}}{(k\tilde{u})^2} \right]. \quad (5.42)$$

The integrals in  $f_1^\mu$  and  $f_2^{\mu\nu}$  can be solved by firstly going from a 4-dimensional to a 3-dimensional integral using (5.30) and then expanding this integral in a parallel and perpendicular part (to the direction of propagation)

$$\frac{d^4p}{(2\pi)^4}F(p) = \frac{d^3\mathbf{p}}{(2\pi)^3\gamma}f(\mathbf{p}) = \frac{d|\mathbf{p}|d^2p_\perp}{(2\pi)^3\gamma}f(\mathbf{p}). \quad (5.43)$$

$\tilde{u}$  is the velocity in the rest frame of the plasma and is equal to (1,0,0,0). Giving us  $k\tilde{u} = \omega$ . We can also express  $ku = \gamma(\omega - \mathbf{k} \cdot \mathbf{v}) = \gamma|\mathbf{k}|(z - \beta \cos \theta)$  with  $z = \omega/|\mathbf{k}|$ ,  $\beta = |\mathbf{b}|$ ,  $|\mathbf{p}| = m\gamma\beta$  ( $d|\mathbf{p}| = m\gamma^3 d\beta$ ) and  $u^\mu = \gamma(\tilde{u}^\mu + \beta b^\mu)$ . Substituting all this into  $f_1^\mu$  and  $f_2^{\mu\nu}$  results in

$$\begin{aligned} f_1^\mu &= z \int_{-\infty}^{\infty} \frac{d|\mathbf{p}|d^2p_\perp}{(2\pi)^3\gamma} (2\pi)^3 \delta^2(p_\perp) g(\gamma) \frac{\tilde{u}^\mu + \beta b^\mu}{z - \beta \cos \theta} \\ &= z \int_{-\infty}^{\infty} \frac{d|\mathbf{p}|}{\gamma} g(\gamma) \frac{\tilde{u}^\mu + \beta b^\mu}{z - \beta} = -zm \int_{-1}^1 d\beta \gamma^2 g(\gamma) \frac{\tilde{u}^\mu + \beta b^\mu}{\beta - z}, \end{aligned} \quad (5.44)$$

and similarly for  $f_2^{\mu\nu}$

$$f_2^{\mu\nu} = z^2 m \int d\beta \gamma^2 g(\gamma) \frac{(\tilde{u}^\mu + \beta b^\mu)(\tilde{u}^\nu + \beta b^\nu)}{(\beta - z)^2}. \quad (5.45)$$

Here the expression for  $f(\mathbf{p})$  has been used. The remaining integrals can be solved using elementary methods for  $g(\gamma) = \frac{ne^{-\rho\gamma}}{2mK_1(\rho)}$  as in the Jüttner distribution. Let us begin with  $f_1^\mu$

$$\begin{aligned} f_1^\mu &= -\frac{zn}{2K_1(\rho)} \int_{-1}^1 d\beta \gamma^2 e^{-\rho\gamma} \frac{\tilde{u}^\mu + \beta b^\mu}{\beta - z} \\ &= -\frac{zn}{2K_1(\rho)} \int_{-1}^1 d\beta \gamma^2 e^{-\rho\gamma} \left[ \frac{1}{\beta - z} \tilde{u}^\mu + \frac{\beta - z + z b^\mu}{\beta - z} \right] \\ &= -\frac{zn}{2K_1(\rho)} \int_{-1}^1 d\beta \left[ \frac{\partial^2}{\partial \rho^2} e^{-\rho\gamma} \frac{1}{\beta - z} \tilde{u}^\mu + \gamma^2 e^{-\rho\gamma} b^\mu + z \frac{\partial^2}{\partial \rho^2} e^{-\rho\gamma} \frac{1}{\beta - z} b^\mu \right]. \end{aligned} \quad (5.46)$$

Using the definition of the MacDonald functions, see Appendix A, with the substitutions  $\gamma = \cosh \chi$  and  $\beta = \tanh \chi$  the second term can be written as

$$\int_{-1}^1 d\beta \gamma^2 e^{-\rho\gamma} = \int_{-\infty}^{\infty} d\chi \frac{\cosh^2 \chi}{\cosh^2 \chi} e^{-\rho \cosh \chi} = 2 \int_0^{\infty} d\chi e^{-\rho \cosh \chi} = 2K_0(\rho). \quad (5.47)$$

Now, remembering the definition of the RPDF (5.37) the final expression for  $f_1^\mu$  becomes

$$f_1^\mu = -\frac{zn}{2K_1(\rho)} \left[ \frac{\partial^2 T(z, \rho)}{\partial \rho^2} (\tilde{u}^\mu + z b^\mu) + 2K_0(\rho) b^\mu \right]. \quad (5.48)$$

Similarly for  $f_2^{\mu\nu}$

$$\begin{aligned}
f_2^{\mu\nu} &= \frac{z^2 n}{2K_1(\rho)} \int_{-1}^1 d\beta \gamma^2 e^{-\rho\gamma} \frac{\tilde{u}^\mu \tilde{u}^\nu + \beta(\tilde{u}^\mu b^\nu + \tilde{u}^\nu b^\mu) + \beta^2 b^\mu b^\nu}{(\beta - z)^2} \\
&= \frac{z^2 n}{2K_1(\rho)} \int_{-1}^1 d\beta \gamma^2 e^{-\rho\gamma} \left[ \frac{1}{(\beta - z)^2} \tilde{u}^\mu \tilde{u}^\nu \right. \\
&\quad \left. + \frac{\beta - z + z}{(\beta - z)^2} (\tilde{u}^\mu b^\nu + \tilde{u}^\nu b^\mu) + \frac{\beta^2 - 2\beta z + z^2 + 2\beta z - z^2}{(\beta - z)^2} b^\mu b^\nu \right] \\
&= \frac{z^2 n}{2K_1(\rho)} \int_{-1}^1 d\beta \left[ \frac{\partial^2}{\partial \rho^2} \frac{\partial}{\partial z} e^{-\rho\gamma} \frac{1}{\beta - z} \tilde{u}^\mu \tilde{u}^\nu + \frac{\partial^2}{\partial \rho^2} \left( \frac{1}{\beta - z} + \frac{\partial}{\partial z} \frac{z}{\beta - z} \right) \right. \\
&\quad \left. \times (\tilde{u}^\mu b^\nu + \tilde{u}^\nu b^\mu) + \left( \gamma^2 e^{-\rho\gamma} + \frac{\partial^2}{\partial \rho^2} \frac{2\beta z}{(\beta - z)^2} - \frac{\partial^2}{\partial \rho^2} \frac{\partial}{\partial z} \frac{z^2}{\beta - z} \right) b^\mu b^\nu \right].
\end{aligned} \tag{5.49}$$

The third to last term is equal to the zeroth order MacDonald function. The second to last term must be rewritten

$$\begin{aligned}
2 \frac{\partial^2}{\partial \rho^2} \int_{-1}^1 d\beta \frac{\beta z}{(\beta - z)^2} b^\mu b^\nu &= 2 \frac{\partial^2}{\partial \rho^2} \int_{-1}^1 d\beta \frac{z(\beta - z) + z^2}{(\beta - z)^2} b^\mu b^\nu \\
&= 2 \frac{\partial^2}{\partial \rho^2} \int_{-1}^1 d\beta \left( z \frac{1}{\beta - z} + z^2 \frac{\partial}{\partial z} \frac{1}{\beta - z} \right) b^\mu b^\nu.
\end{aligned} \tag{5.50}$$

Adding all this together and using the definition of the RPDF (5.37)  $f_2^{\mu\nu}$  becomes

$$\begin{aligned}
f_2^{\mu\nu} &= \frac{nz^2}{2K_1(\rho)} \left\{ \frac{\partial T(z, \rho)}{\partial \rho^2} (\tilde{u}^\mu + zb^\mu)(\tilde{u}^{\nu\mu} + zb^\nu) \right. \\
&\quad \left. + \frac{\partial^2 T(z, \rho)}{\partial \rho^2} [(\tilde{u}^\mu b^\nu + \tilde{u}^\nu b^\mu) + 2zb^\mu b^\nu] + 2K_0(\rho) b^\mu b^\nu \right\}.
\end{aligned} \tag{5.51}$$

Thus the LRT for a strictly-parallel distribution is

$$\Pi^{\mu\nu}(k) = -\frac{q^2}{m} \left[ n_{pr} g^{\mu\nu} - \frac{k^\mu f_1^\nu + k^\nu f_1^\mu}{k\tilde{u}} + \frac{k^2 f_2^{\mu\nu}}{(k\tilde{u})^2} \right], \tag{5.52}$$

where

$$f_1^\mu = \frac{-nz}{2K_1(\rho)} \left[ \frac{\partial^2 T(z, \rho)}{\partial \rho^2} (\tilde{u}^\mu + zb^\mu) + 2K_0(\rho) b^\mu \right], \tag{5.53}$$

and

$$\begin{aligned}
f_2^{\mu\nu} &= \frac{nz^2}{2K_1(\rho)} \left\{ \frac{\partial T(z, \rho)}{\partial \rho^2} (\tilde{u}^\mu + zb^\mu)(\tilde{u}^{\nu\mu} + zb^\nu) \right. \\
&\quad \left. + \frac{\partial^2 T(z, \rho)}{\partial \rho^2} [(\tilde{u}^\mu b^\nu + \tilde{u}^\nu b^\mu) + 2zb^\mu b^\nu] + 2K_0(\rho) \right\}.
\end{aligned} \tag{5.54}$$

# 6 — Absorption Coefficient for the Jüttner Particle Distribution

With the linear response tensor calculated in the previous chapter we can calculate the absorption coefficient for the plasma. In this chapter the absorption coefficient will be calculated for the Jüttner distribution. It will be a function of the phase velocity  $z$ , the relativistic factor  $\rho$  and the ratio of the plasma frequency and the frequency of the longitudinal wave mode  $x \equiv \omega_p/\omega_L$ . From plots of the absorption coefficient it will be clear that there are some problems with the results which are discussed. At the end of the chapter the absorption coefficient will be recalculated with a different LRT taken from Ref [15].

## 6.1 Absorption Coefficient for the Jüttner Distribution

The longitudinal part of the response tensor is

$$\begin{aligned}\Pi_L &= e_L^\mu \Pi_{\mu\nu} e_L^\nu = \left(1 - \frac{\omega^2}{k^2}\right) \Pi^{00} = \left(1 - \frac{\omega^2}{\omega^2 - |\mathbf{k}|^2}\right) \Pi^{00} \\ &= \left(1 - \frac{1}{1 - z^{-2}}\right) \Pi^{00} = \left(\frac{1 - z^{-2} - 1}{1 - z^{-2}}\right) \Pi^{00} = \frac{1}{1 - z^2} \Pi^{00}.\end{aligned}\quad (6.1)$$

The expression for the longitudinal part is from Ref [21]. We choose the electron-positron beam and the emitted photon mode to be in the  $z$ -direction, that is  $k = (\omega, 0, 0, k)$  and  $b = (0, 0, 0, 1)$ . Also note that  $\tilde{u} = (1, 0, 0, 0)$  is the velocity in the rest frame. The 00-component of the LRT (5.52) is

$$\begin{aligned}\Pi^{00} &= -\frac{q^2}{m} \left[ n_{pr} g^{00} - \frac{k^0 f_1^0 + k^0 f_1^0}{k\tilde{u}} + \frac{k^2 f_2^{00}}{(k\tilde{u})} \right] \\ &= -\frac{q^2}{m} \left[ n_{pr} - \frac{\omega f_1^0 + \omega f_1^0}{\omega} + \frac{(\omega^2 - |\mathbf{k}|^2) f_2^{00}}{\omega^2} \right] \\ &= -\frac{q^2}{m} \left[ n_{pr} - 2f_1^0 + \left(1 - \frac{|\mathbf{k}|^2}{\omega^2}\right) f_2^{00} \right] \\ &= -\frac{q^2}{m} \left[ n_{pr} - 2f_1^0 + (1 - z^{-2}) f_2^{00} \right].\end{aligned}\quad (6.2)$$

The zeroth components of  $f_1^\mu$  (5.53) and  $f_2^{\mu\nu}$  (5.54) are

$$f_1^0 = -\frac{nz}{2K_1(\rho)} \left[ (\tilde{u}^0 + zb^0) \frac{\partial^2 T(z, \rho)}{\partial \rho^2} + b^0 2K_0(\rho) \right] = -\frac{n\omega}{2K_1(\rho)|\mathbf{k}|} \frac{\partial^2 T(z, \rho)}{\partial \rho^2}, \quad (6.3)$$

and

$$\begin{aligned} f_2^{00} &= \frac{nz^2}{2K_1(\rho)} \left[ (\tilde{u}^0 + zb^0)(\tilde{u}^0 + zb^0) \frac{\partial^2 T'(z, \rho)}{\partial \rho^2} + (\tilde{u}^0 b^0 + \tilde{u}^0 b^0 + 2zb^0 b^0) \frac{\partial^2 T(z, \rho)}{\partial \rho^2} + b^0 b^0 2K_0(\rho) \right] \\ &= \frac{n\omega^2}{2K_1(\rho)|\mathbf{k}|^2} \frac{\partial^2 T'(z, \rho)}{\partial \rho^2}, \end{aligned} \quad (6.4)$$

where the prime indicates a derivative with respect to  $z$ . With this the 00-component of the LRT is

$$\begin{aligned} \Pi^{00} &= -\frac{q^2}{m} \left[ n_{\text{pr}} + 2 \frac{nz}{2K_1(\rho)} \frac{\partial^2 T(z, \rho)}{\partial \rho^2} + (1 - z^{-2}) \frac{nz^2}{2K_1(\rho)} \frac{\partial^2 T'(z, \rho)}{\partial \rho^2} \right] \\ &= -\frac{q^2}{m} \left[ n_{\text{pr}} + \frac{nz}{K_1(\rho)} \frac{\partial^2 T(z, \rho)}{\partial \rho^2} + (z^2 - 1) \frac{n}{2K_1(\rho)} \frac{\partial^2 T'(z, \rho)}{\partial \rho^2} \right]. \end{aligned} \quad (6.5)$$

In order to get a slightly simpler expression we use the relation  $n_{\text{pr}} = n \frac{K_1(\rho)}{K_2(\rho)}$  and rewrite to

$$\Pi^{00} = -\frac{q^2 n}{m} \left[ \frac{K_1(\rho)}{K_2(\rho)} + \frac{z}{K_1(\rho)} \frac{\partial^2 T(z, \rho)}{\partial \rho^2} - \frac{1 - z^2}{2K_1(\rho)} \frac{\partial^2 T'(z, \rho)}{\partial \rho^2} \right]. \quad (6.6)$$

It is useful to split this into a real and imaginary part, namely

$$\text{Re}\Pi^{00} = -\frac{q^2 n}{m} \left[ \frac{K_1(\rho)}{K_2(\rho)} + \frac{z}{K_1(\rho)} \text{Re} \frac{\partial^2 T(z, \rho)}{\partial \rho^2} - \frac{1 - z^2}{2K_1(\rho)} \text{Re} \frac{\partial^2 T'(z, \rho)}{\partial \rho^2} \right], \quad (6.7)$$

and

$$\text{Im}\Pi^{00} = -\frac{q^2 n}{2mK_1(\rho)} \left[ 2z \text{Im} \frac{\partial^2 T(z, \rho)}{\partial \rho^2} - (1 - z^2) \text{Im} \frac{\partial^2 T'(z, \rho)}{\partial \rho^2} \right]. \quad (6.8)$$

We will have use for the derivative of the real part with respect to  $\omega$ . Since it is easier to work with the derivative with respect to  $z$  we rewrite the derivative using that the two derivatives are connected by  $\frac{\partial}{\partial \omega} = \frac{\partial z}{\partial \omega} \frac{\partial}{\partial z} = \frac{1}{|\mathbf{k}|} \frac{\partial}{\partial z}$ . The derivative of the real part of  $\Pi^{00}$  with respect to  $z$  is

$$\begin{aligned} \frac{\partial}{\partial z} \text{Re}\Pi^{00} &= \frac{\partial}{\partial z} \left( -\frac{q^2 n}{m} \right) \left[ \frac{K_1(\rho)}{K_2(\rho)} + \frac{z}{K_1(\rho)} \text{Re} \frac{\partial^2 T(z, \rho)}{\partial \rho^2} - \frac{1 - z^2}{2K_1(\rho)} \text{Re} \frac{\partial^2 T'(z, \rho)}{\partial \rho^2} \right] \\ &= -\frac{q^2 n}{m} \left[ \frac{1}{K_1(\rho)} \text{Re} \frac{\partial^2 T(z, \rho)}{\partial \rho^2} + \frac{z}{K_1(\rho)} \frac{\partial^2 T'(z, \rho)}{\partial \rho^2} + \frac{z}{K_1(\rho)} \text{Re} \frac{\partial^2 T'(z, \rho)}{\partial \rho^2} \right. \\ &\quad \left. - \frac{1 - z^2}{2} \text{Re} \frac{\partial^2 T''(z, \rho)}{\partial \rho^2} \right] \\ &= -\frac{q^2 n}{2mK_1(\rho)} \left[ 2 \text{Re} \frac{\partial^2 T(z, \rho)}{\partial \rho^2} + 4z \text{Re} \frac{\partial^2 T'(z, \rho)}{\partial \rho^2} - (1 - z^2) \frac{\partial^2 T''(z, \rho)}{\partial \rho^2} \right]. \end{aligned} \quad (6.9)$$

In order to find the growth rate (4.38) one needs a factor  $R_L$  (4.25) which is

$$[R_L]^{-1} = - \left[ \frac{1}{\omega} \frac{\partial}{\partial \omega} \Lambda_L \right] \Big|_{\omega=\omega_L}, \quad (6.10)$$

where  $\Lambda_L(k) = e_{L,\mu}\Lambda^{H\mu\nu}(k)e_{L,\nu}$  with  $\Lambda^{\mu\nu}(k) = k^2g^{\mu\nu} - k^\mu k^\nu + \mu_0\Pi^{\mu\nu}(k)$ . The Hermitian part of the tensor is equal to real part of the tensor since the tensor is symmetric (in the same way the anti-Hermitian part is equal to the imaginary part). This gives

$$\begin{aligned}\frac{\partial}{\partial\omega}\Lambda_L &= \frac{\partial}{\partial\omega}\left[k^2(e_L \cdot e_L) - (k \cdot e_L)(k \cdot e_L) + \mu_0\text{Re}\Pi_L\right] \\ &= \frac{\partial}{\partial\omega}(-\omega^2 - |\mathbf{k}|^2) + \mu_0\frac{\partial}{\partial\omega}\text{Re}\Pi_L \\ &= -2\omega + \mu_0\frac{\partial}{\partial\omega}\text{Re}\Pi_L.\end{aligned}\tag{6.11}$$

The last derivative in this equation is solved by rewriting the derivative to one with respect to  $z$  as before and using the result from equation (6.9)

$$\begin{aligned}\frac{\partial}{\partial\omega}\text{Re}\Pi_L &= \frac{1}{|\mathbf{k}|}\frac{\partial}{\partial z}\left[\frac{1}{1-z^2}\text{Re}\Pi^{00}\right] \\ &= \frac{1}{|\mathbf{k}|}\left[\frac{2z}{(1-z^2)^2}\text{Re}\Pi^{00} + \frac{1}{1-z^2}\frac{\partial}{\partial z}\text{Re}\Pi^{00}\right].\end{aligned}\tag{6.12}$$

With this  $\frac{\partial}{\partial\omega}\Lambda_L$  becomes

$$\begin{aligned}\frac{\partial}{\partial\omega}\Lambda_L &= -2\omega + \frac{\mu_0}{|\mathbf{k}|}\left\{\frac{2z}{(1-z^2)^2}\left(-\frac{q^2n}{m}\right)\left[\frac{K_1(\rho)}{K_2(\rho)} + \frac{z}{K_1(\rho)}\text{Re}\frac{\partial^2T(z,\rho)}{\partial\rho^2}\right.\right. \\ &\quad \left.\left.-\frac{1-z^2}{2K_1(\rho)}\text{Re}\frac{\partial^2T'(z,\rho)}{\partial\rho^2}\right] + \frac{1}{z^2}\left(-\frac{q^2n}{2mK_1(\rho)}\right)\left[2\text{Re}\frac{\partial^2T(z,\rho)}{\partial\rho^2}\right.\right. \\ &\quad \left.\left.+4z\text{Re}\frac{\partial^2T'(z,\rho)}{\partial\rho^2} - (1-z^2)\text{Re}\frac{\partial^2T''(z,\rho)}{\partial\rho^2}\right]\right\} \\ &= -2\omega - \frac{\epsilon_0\mu_0q^2n}{\epsilon_0|\mathbf{k}|m(1-z^2)}\text{Re}\left[\frac{2z}{1-z^2}\left(\frac{K_1(\rho)}{K_2(\rho)} + \frac{z}{K_1(\rho)}\frac{\partial^2T(z,\rho)}{\partial\rho^2} - \frac{1-z^2}{2K_1(\rho)}\frac{\partial^2T'(z,\rho)}{\partial\rho^2}\right)\right. \\ &\quad \left.+ \frac{1}{2K_1(\rho)}\left(2\frac{\partial^2T(z,\rho)}{\partial\rho^2} + 4z\frac{\partial^2T'(z,\rho)}{\partial\rho^2} - (1-z^2)\frac{\partial^2T''(z,\rho)}{\partial\rho^2}\right)\right] \\ &= -2\omega - \frac{\omega_p^2z}{\omega(1-z^2)}\text{Re}\left[\frac{2z}{1-z^2}\left(\frac{K_1(\rho)}{K_2(\rho)} + \frac{z}{K_1(\rho)}\frac{\partial^2T(z,\rho)}{\partial\rho^2} - \frac{1-z^2}{2K_1(\rho)}\frac{\partial^2T'(z,\rho)}{\partial\rho^2}\right)\right. \\ &\quad \left.+ \frac{1}{2K_1(\rho)}\left(2\frac{\partial^2T(z,\rho)}{\partial\rho^2} + 4z\frac{\partial^2T'(z,\rho)}{\partial\rho^2} - (1-z^2)\frac{\partial^2T''(z,\rho)}{\partial\rho^2}\right)\right].\end{aligned}\tag{6.13}$$

Here we have used the relation  $\epsilon_0\mu_0 = c^{-2} = 1$ , which is true when we are working in natural units, and we have introduced the plasma frequency  $\omega_p = \sqrt{\frac{q^2n}{\epsilon_0m}}$ . All the elements of  $R_L$  are now known and it is expressed as

$$\begin{aligned}R_L^{-1} &= -\left[\frac{1}{\omega}\frac{\partial}{\partial\omega}\Lambda_L\right]\Bigg|_{\omega=\omega_L} \\ &= 2 + \frac{\omega_p^2z}{\omega_L^2(1-z^2)}\text{Re}\left[\frac{2z}{1-z^2}\left(\frac{K_1(\rho)}{K_2(\rho)} + \frac{z}{K_1(\rho)}\frac{\partial^2T(z,\rho)}{\partial\rho^2} - \frac{1-z^2}{2K_1(\rho)}\frac{\partial^2T'(z,\rho)}{\partial\rho^2}\right)\right. \\ &\quad \left.+ \frac{1}{2K_1(\rho)}\left(2\frac{\partial^2T(z,\rho)}{\partial\rho^2} + 4z\frac{\partial^2T'(z,\rho)}{\partial\rho^2} - (1-z^2)\frac{\partial^2T''(z,\rho)}{\partial\rho^2}\right)\right].\end{aligned}\tag{6.14}$$

The last part needed is  $\Pi_L^A$  which is found using the imaginary part of the 00-component of the response tensor

$$\begin{aligned}\Pi_L^A &= \left( \frac{1}{1-z^2} \right) \Pi^{A,00} = (1-z^2)^{-1} i \text{Im}[\Pi^{00}] \\ &= - \frac{iq^2 n}{2K_1(\rho)m(1-z^2)} \text{Im} \left[ 2z \frac{\partial^2 T(z, \rho)}{\partial \rho^2} - (1-z^2) \frac{\partial^2 T'(z, \rho)}{\partial \rho^2} \right].\end{aligned}\tag{6.15}$$

Now we have everything we need to calculate the absorption coefficient for the Jüttner distribution in terms of the derivatives of the relativistic plasma dispersion function. From the definition in equation (4.38) the absorption coefficient is

$$\begin{aligned}\gamma_L &= 2i \frac{R_L}{\epsilon_0 \omega_L} \Pi_L^A \\ &= - \frac{2i}{\epsilon_0 \omega_L} \frac{iq^2 n}{2K_1(\rho)m(1-z^2)} \text{Im} \left[ 2z \frac{\partial^2 T(z, \rho)}{\partial \rho^2} - (1-z^2) \frac{\partial^2 T'(z, \rho)}{\partial \rho^2} \right] \\ &\times \left\{ 2 + \frac{\omega_p^2 z}{\omega_L^2 (1-z^2)} \text{Re} \left[ \frac{2z}{1-z^2} \left( \frac{K_1(\rho)}{K_2(\rho)} + \frac{z}{K_1(\rho)} \frac{\partial^2 T(z, \rho)}{\partial \rho^2} - \frac{1-z^2}{2K_1(\rho)} \frac{\partial^2 T'(z, \rho)}{\partial \rho^2} \right) \right. \right. \\ &\left. \left. + \frac{1}{2K_1(\rho)} \left( 2 \frac{\partial^2 T(z, \rho)}{\partial \rho^2} + 4z \frac{\partial^2 T'(z, \rho)}{\partial \rho^2} - (1-z^2) \frac{\partial^2 T''(z, \rho)}{\partial \rho^2} \right) \right] \right\}^{-1} \\ &= \frac{\omega_p^2}{\omega_L K_1(\rho)(1-z^2)} \text{Im} \left[ 2z \frac{\partial^2 T(z, \rho)}{\partial \rho^2} - (1-z^2) \frac{\partial^2 T'(z, \rho)}{\partial \rho^2} \right] \\ &\times \left\{ 2 + \frac{\omega_p^2 z}{\omega_L^2 (1-z^2)} \text{Re} \left[ \frac{2z}{1-z^2} \left( \frac{K_1(\rho)}{K_2(\rho)} + \frac{z}{K_1(\rho)} \frac{\partial^2 T(z, \rho)}{\partial \rho^2} - \frac{1-z^2}{2K_1(\rho)} \frac{\partial^2 T'(z, \rho)}{\partial \rho^2} \right) \right. \right. \\ &\left. \left. + \frac{1}{2K_1(\rho)} \left( 2 \frac{\partial^2 T(z, \rho)}{\partial \rho^2} + 4z \frac{\partial^2 T'(z, \rho)}{\partial \rho^2} - (1-z^2) \frac{\partial^2 T''(z, \rho)}{\partial \rho^2} \right) \right] \right\}^{-1}.\end{aligned}\tag{6.16}$$

There are three variables present in the absorption coefficient (6.16). They are the phase velocity  $z$ , the ratio of the plasma frequency and the frequency of the longitudinal wave mode  $x$  and the relativistic factor  $\rho = m/T$ . Let us look at the absorption coefficient in three regions of  $\rho$ . Namely  $\rho = 0.01$  in Figure 6.1  $\rho = 1$  in Figure 6.2 and  $\rho = 100$  in Figure 6.3. This is the ultrarelativistic, relativistic and classical limit, respectively. They are all plotted with a frequency ratio of  $x = 4$ . Note that for different values of  $x$  the absorption coefficients look completely different and the value 4 holds no special significance and the plots are therefore just examples of the absorption coefficient.

All of these absorption coefficients are complicated with divergences to both plus and minus infinity. For other values of  $x$  these divergences disappear and the absorption coefficient becomes positive. The divergences arise from the factor  $R_L$  which becomes zero for certain values of  $z$ ,  $\rho$  and  $x$ .

It is instructive to split the absorption coefficient into  $\Pi_L$  with prefactors and  $R_L$ . This is shown in figure 6.4, where it can be seen that  $\Pi_L$  with prefactors is positive and the negative values in the absorption coefficient appears when  $R_L$  turns negative. This is true for all values of  $z$ ,  $\rho$  and  $x$ . To see that  $\Pi_L$  with prefactors are



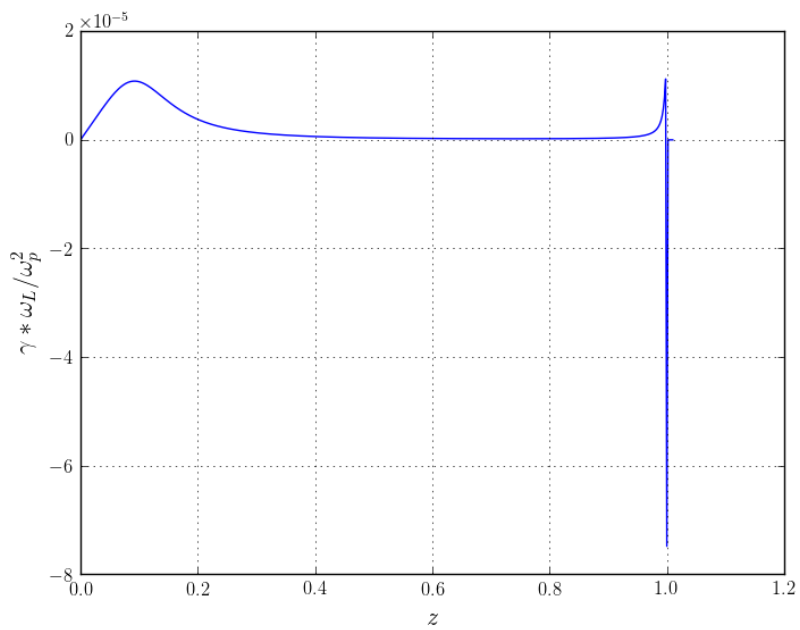


Figure 6.1: The figure shows the absorption coefficient as a function of  $z$  for  $\rho = 0.01$  and  $x = 4$ . It is positive, stable, until  $z$  gets close to 1 where it becomes negative, unstable.

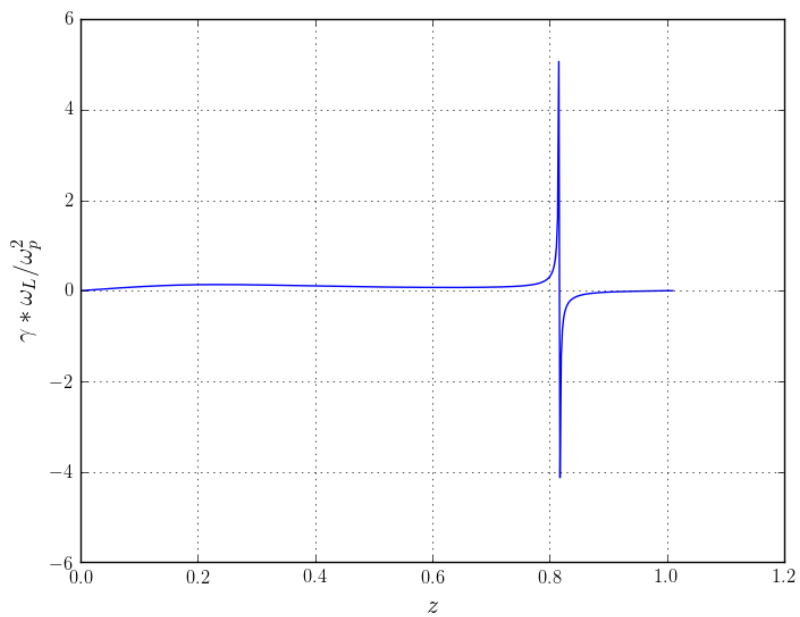


Figure 6.2: The figure shows the absorption coefficient as a function of  $z$  for  $\rho = 1$  and  $x = 4$ . It is positive, stable, until it diverges and negative, unstable, after.

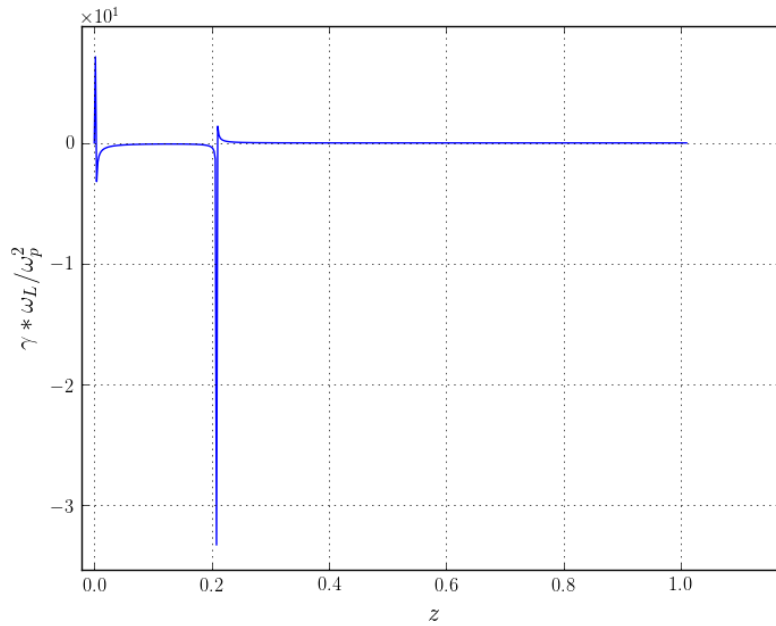


Figure 6.3: The figure shows the absorption coefficient as a function of  $z$  for  $\rho = 100$  and  $x = 4$ . It is positive, stable, for very small values of  $z$  then it diverges and becomes negative, unstable, before it diverges again and becomes positive.

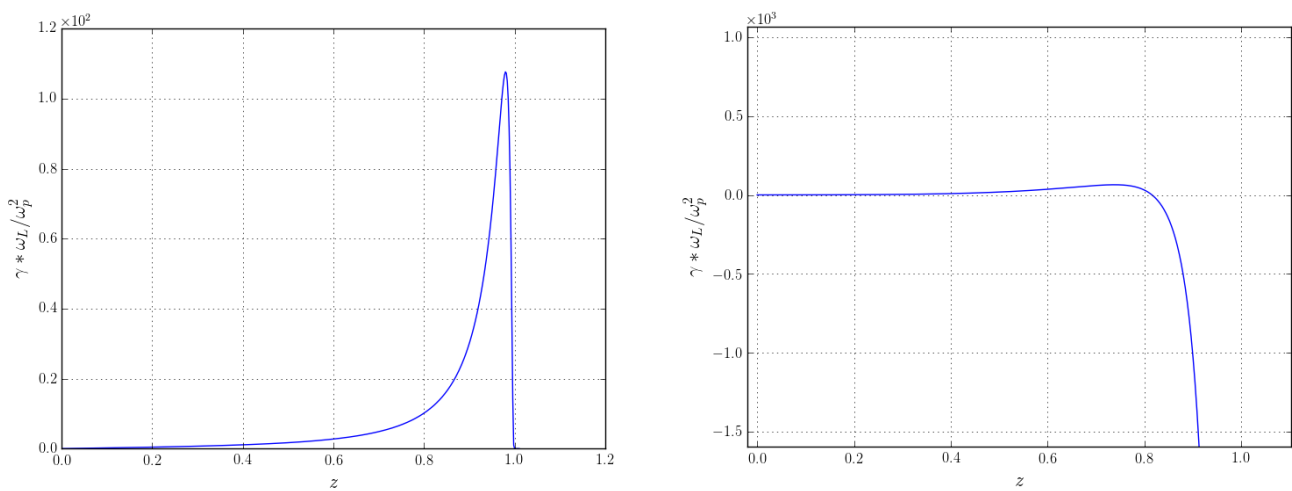


Figure 6.4: The figure shows  $\Pi_L$  with prefactors and  $R_L$  as a function of  $z$  for  $\rho = 1$  and  $x = 4$ . One can see that  $\Pi_L$  with prefactors is always positive while  $R_L$  takes both positive and negative values.

positive we look at

$$\frac{2\omega_p^2}{\omega_L K_1(\rho)(1-z^2)} \text{Im} \left[ 2z \frac{\partial^2 T(z, \rho)}{\partial \rho^2} - (1-z^2) \frac{\partial^2 T'(z, \rho)}{\partial \rho^2} \right]. \quad (6.17)$$

The factors before the imaginary part are positive,  $K_1(\rho) > 0$  is shown in Appendix A, so the total expression is positive if the imaginary part is positive.  $\frac{\partial^2 T(z, \rho)}{\partial \rho^2}$  and  $\frac{\partial^2 T'(z, \rho)}{\partial \rho^2}$  are written explicitly in appendix B and the imaginary part is

$$\begin{aligned} & \text{Im} \left[ 2z \frac{\partial^2 T(z, \rho)}{\partial \rho^2} - (1-z^2) \frac{\partial^2 T'(z, \rho)}{\partial \rho^2} \right] \\ &= \pi \gamma_0^3 z \rho e^{-\rho \gamma_0}, \end{aligned} \quad (6.18)$$

which is positive. The criterion for an instability hence becomes  $R_L \leq 0$ , or

$$\begin{aligned} -2 \geq & \frac{\omega_p^2 z}{\omega_L^2 (1-z^2)} \text{Re} \left[ \frac{2z}{1-z^2} \left( \frac{K_1(\rho)}{K_2(\rho)} + \frac{z}{K_1(\rho)} \frac{\partial^2 T(z, \rho)}{\partial \rho^2} - \frac{1-z^2}{2K_1(\rho)} \frac{\partial^2 T'(z, \rho)}{\partial \rho^2} \right) \right. \\ & \left. + \frac{1}{2K_1(\rho)} \left( 2 \frac{\partial^2 T(z, \rho)}{\partial \rho^2} + 4z \frac{\partial^2 T'(z, \rho)}{\partial \rho^2} - (1-z^2) \frac{\partial^2 T''(z, \rho)}{\partial \rho^2} \right) \right]. \end{aligned} \quad (6.19)$$

The goal of this thesis has been to find out if the growth rate of the plasma was such that the time scale of the energy dissipation could compete with that of the inverse Compton cascade. To do this we would need the maximum value of the growth rate. Since the absorption coefficient shown here diverges to minus infinity the maximum value is formally infinite. This is not physical and one must conclude that the divergences are a result of the way the calculations have been done and should be corrected. The error most likely occurs when Plemelj's formula has been applied in separating the LRT into an imaginary and a real part. This separation is not made clear in this chapter, but is more easily understood in the next one. In the relativistic particle dispersion relation (5.37) there is a pole at  $\beta = z$ . Using Plemelj's formula this is split into a real principle value integral and an imaginary part as follows

$$\frac{1}{x-a+0i} = \mathcal{P} \left( \frac{1}{x-a} \right) - i\pi \delta(x-a). \quad (6.20)$$

This, however, requires the imaginary part of the frequency, known as the absorption coefficient, to be small. As the imaginary part diverges in the absorption coefficient, seen in Figures 6.1, 6.2 and 6.3, this assumption is clearly not valid anymore and the method is not self-consistent.

## 6.2 Alternative Absorption Coefficient for the Jüttner Distribution

A different expression for the LRT is found in Ref [15]. It is

$$\Pi^{\mu\nu}(k) = 16\pi\alpha \int \frac{d^3p}{(2\pi)^3} \frac{1}{2E} f(p) \frac{p \cdot k (p^\mu k^\nu + k^\mu p^\nu) - k^2 p^\mu p^\nu - (p \cdot k)^2 g^{\mu\nu}}{(p \cdot k)^2 - (k^2)^2/4}. \quad (6.21)$$

From this expression we can again calculate the response tensor with a Jüttner particle distribution. Start by using the approximation  $(k^2)^2 \approx 0$  following Ref [15] and let the momentum and wavenumber be parallel in the z-direction,  $p = (E, 0, 0, p)$  and  $k = (\omega, 0, 0, k)$ , resulting in

$$\begin{aligned}\Pi^{00} &= 16\pi\alpha \int \frac{d^3p}{(2\pi)^3} \frac{1}{2E} f(p) \frac{2\omega(\omega - \beta k) - (\omega^2 - k^2) - (\omega - \beta k)^2}{(\omega - \beta k)^2} \\ &= 16\pi\alpha \int \frac{d^3p}{(2\pi)^3} \frac{1}{2E} f(p) \frac{2\omega^2 - 2\omega\beta k - \omega^2 + k^2 - \omega^2 + 2\omega\beta k - \beta^2 k^2}{(\omega - \beta k)^2} \\ &= 16\pi\alpha \int \frac{d^3p}{(2\pi)^3} \frac{1}{2E} f(p) \frac{k^2(1 - \beta^2)}{(\omega - \beta k)^2}.\end{aligned}\quad (6.22)$$

Inserting the Jüttner distribution

$$f(p) = (2\pi)^3 \delta(p_x) \delta(p_y) \frac{ne^{-\rho\gamma}}{2mK_1(\rho)}, \quad (6.23)$$

$E = m\gamma$ ,  $dp = d\beta m\gamma^3$  and  $\alpha = q^2/4\pi$  the 00-component response tensor becomes

$$\begin{aligned}\Pi^{00} &= \frac{8\pi\alpha n}{2mK_1(\rho)} \int dp_z \frac{1}{E} \frac{k^2(1 - \beta^2)}{(\omega - \beta k)^2} e^{-\rho\gamma} \\ &= \frac{4\pi\alpha n}{mK_1(\rho)} \int d\beta m\gamma^3 \frac{1}{E} \frac{1 - \beta^2}{(\beta - z)^2} \\ &= \frac{4\pi\alpha n}{mK_1(\rho)} \int d\beta \gamma^2 \frac{1 - \beta^2}{(\beta - z)^2} \\ &= \frac{4\pi\alpha n}{mK_1(\rho)} \left[ \frac{\partial}{\partial z} \frac{\partial^2}{\partial \rho^2} \int d\beta \frac{1}{\beta - z} e^{-\rho\gamma} - \int d\beta \gamma^2 \frac{\beta^2}{(\beta - z)^2} e^{-\rho\gamma} \right].\end{aligned}$$

As before we employ the integral technique of adding zero,  $z - z$ , to the integrand and recognize the integrals as derivatives of the relativistic particle dispersion relation. This yields

$$\begin{aligned}\Pi^{00} &= \frac{4\pi\alpha n}{mK_1(\rho)} \left[ \frac{\partial^2 T'(z, \rho)}{\partial \rho^2} - \int d\beta \gamma \frac{\beta^2 - z^2 + z^2}{(\beta - z)^2} e^{-\rho\gamma} \right] \\ &= \frac{4\pi\alpha n}{mK_1(\rho)} \left[ \frac{\partial^2 T'(z, \rho)}{\partial \rho^2} - \int d\beta \gamma \frac{(\beta + z)(\beta - z) + z^2}{(\beta - z)^2} e^{-\rho\gamma} \right] \\ &= \frac{4\pi\alpha n}{mK_1(\rho)} \left[ \frac{\partial^2 T'(z, \rho)}{\partial \rho^2} - \int d\beta \gamma^2 \frac{\beta + z}{\beta - z} e^{-\rho\gamma} - \int d\beta \gamma^2 \frac{z^2}{(\beta - z)^2} e^{-\rho\gamma} \right] \\ &= \frac{4\pi\alpha n}{mK_1(\rho)} \left[ \frac{\partial^2 T'(z, \rho)}{\partial \rho^2} - \frac{\partial^2}{\partial \rho^2} zT(z, \rho) - \int d\beta \gamma^2 \frac{\beta - z + z}{\beta - z} e^{-\rho\gamma} - \int d\beta \gamma^2 \frac{z^2}{(\beta - z)^2} e^{-\rho\gamma} \right] \\ &= \frac{4\pi\alpha n}{mK_1(\rho)} \left[ \frac{\partial^2 T'(z, \rho)}{\partial \rho^2} - 2z \frac{\partial^2 T(z, \rho)}{\partial \rho^2} - \int d\beta \gamma^2 e^{-\rho\gamma} - z^2 \frac{\partial^2 T'(z, \rho)}{\partial \rho^2} \right] \\ &= \frac{4\pi\alpha n}{mK_1(\rho)} \left[ \frac{\partial^2 T'(z, \rho)}{\partial \rho^2} - 2z \frac{\partial^2 T(z, \rho)}{\partial \rho^2} - z^2 \frac{\partial^2 T'(z, \rho)}{\partial \rho^2} - 2K_0(\rho) \right] \\ &= -\frac{q^2 n}{mK_1(\rho)} \left[ 2z \frac{\partial^2 T(z, \rho)}{\partial \rho^2} - (1 - z^2) \frac{\partial^2 T'(z, \rho)}{\partial \rho^2} + 2K_0(\rho) \right].\end{aligned}\quad (6.24)$$

This expression is very similar to (6.6). The only difference is a factor 2 and the term consisting of MacDonald functions has changed from  $K_1(\rho)/K_2(\rho)$  to  $K_0(\rho)/K_1(\rho)$ . As a result the absorption coefficient is also very similar,

$$\begin{aligned}
 \gamma_L &= 2i \frac{R_L}{\epsilon_0 \omega_L} \Pi_L^A \\
 &= -\frac{2i}{\epsilon_0 \omega_L} \frac{2iq^2 n}{2K_1(\rho)m(1-z^2)} \operatorname{Im} \left[ 2z \frac{\partial^2 T(z, \rho)}{\partial \rho^2} - (1-z^2) \frac{\partial^2 T'(z, \rho)}{\partial \rho^2} \right] \\
 &\times \left\{ 2 + \frac{2\omega_p^2 z}{\omega_L^2 (1-z^2)} \operatorname{Re} \left[ \frac{2z}{1-z^2} \left( \frac{K_0(\rho)}{K_1(\rho)} + \frac{z}{K_1(\rho)} \frac{\partial^2 T(z, \rho)}{\partial \rho^2} - \frac{1-z^2}{2K_1(\rho)} \frac{\partial^2 T'(z, \rho)}{\partial \rho^2} \right) \right. \right. \\
 &\left. \left. + \frac{1}{2K_1(\rho)} \left( 2 \frac{\partial^2 T(z, \rho)}{\partial \rho^2} + 4z \frac{\partial^2 T'(z, \rho)}{\partial \rho^2} - (1-z^2) \frac{\partial^2 T''(z, \rho)}{\partial \rho^2} \right) \right] \right\}^{-1} \\
 &= \frac{2\omega_p^2}{\omega_L K_1(\rho)(1-z^2)} \operatorname{Im} \left[ 2z \frac{\partial^2 T(z, \rho)}{\partial \rho^2} - (1-z^2) \frac{\partial^2 T'(z, \rho)}{\partial \rho^2} \right] \\
 &\times \left\{ 2 + \frac{2\omega_p^2 z}{\omega_L^2 (1-z^2)} \operatorname{Re} \left[ \frac{2z}{1-z^2} \left( \frac{K_0(\rho)}{K_1(\rho)} + \frac{z}{K_1(\rho)} \frac{\partial^2 T(z, \rho)}{\partial \rho^2} - \frac{1-z^2}{2K_1(\rho)} \frac{\partial^2 T'(z, \rho)}{\partial \rho^2} \right) \right. \right. \\
 &\left. \left. + \frac{1}{2K_1(\rho)} \left( 2 \frac{\partial^2 T(z, \rho)}{\partial \rho^2} + 4z \frac{\partial^2 T'(z, \rho)}{\partial \rho^2} - (1-z^2) \frac{\partial^2 T''(z, \rho)}{\partial \rho^2} \right) \right] \right\}^{-1}, \tag{6.25}
 \end{aligned}$$

which is the same as (6.16), but with the substitutions mentioned above. The difference between these is not known. It could come from the approximation  $(k^2)^2 \approx 0$  or there is a mistake in Refs [14] or [15]. The calculation in the next section is done using the LRT from this section instead of the one used in the last section because it is somewhat simpler.



# 7 — Absorption Coefficient for a Simulated Particle Distribution

In this chapter the absorption coefficient will be recalculated with a distribution function based on a simulation of the electromagnetic cascade described in the introduction [22]. This new distribution function will change the absorption coefficient. Notably the relativistic particle dispersion relation,  $T(z, \rho)$  is no longer present (although a part of the expression has the same form). This means that the integrations over the velocity have to be calculated again and new techniques have to be employed to find the real and imaginary parts of the response tensor. In addition to this we will use the response tensor from Ref [15] instead of Ref [14] as it is somewhat simpler. The chapter will start with the calculation of the absorption coefficient, it will be presented and discussed. Lastly the distribution function and its numerical calculation will be discussed.

## 7.1 Absorption Coefficient for Simulated Distribution Function

The 00-component of the linear response tensor from Ref [15], equation (6.22), was found in the last chapter,

$$\Pi^{00} = 16\pi\alpha \int \frac{d^3p}{(2\pi)^3} \frac{1}{2E} n(E) \frac{k^2(1-\beta^2)}{(\omega - \beta k)^2}. \quad (7.1)$$

This equation contains the distribution function  $n(E)$  which is

$$n(E) = n_0(2\pi)^3 \delta(p_x)\delta(p_y)[\delta(p_z) + Bf(E)H(\beta)]. \quad (7.2)$$

The form of the distribution function will be discussed in the next section. It contains the function  $f(E)$  which is the particle distribution over energy and is based on a simulation of the electromagnetic cascade the plasma beam experiences in the intergalactic medium. Now, with this expression for  $n(E)$  the 00-component

of the LRT becomes

$$\begin{aligned}
 \Pi^{00} &= 16\pi\alpha n_0 \left[ \int d^3p \frac{1}{2E} \delta(p_x) \delta(p_y) \frac{1 - \beta^2}{(z - \beta)^2} [\delta(p_z) + B f(E) H(\beta)] \right] \\
 &= 16\pi\alpha n_0 \left[ \frac{1}{2mz^2} + B \int_{-\infty}^{\infty} dp_z \frac{1}{2m\gamma} \frac{(1 - \beta^2) f(E)}{(z - \beta)^2} H(\beta) \right] \\
 &= 16\pi\alpha n_0 \left[ \frac{1}{2mz^2} + B \int_{-\infty}^{\infty} dp_z \frac{1}{2m\gamma^3} \frac{f(E)}{(z - \beta)^2} H(\beta) \right].
 \end{aligned} \tag{7.3}$$

In order to solve the integrals we do a change of integration variable from momentum to velocity. The variables are connected by  $p_z = m\gamma\beta$  and the derivative is  $dp_z = m\gamma^3 d\beta$ . With this the 00-component of the LRT becomes

$$\begin{aligned}
 \Pi^{00} &= 16\pi\alpha n_0 \left[ \frac{1}{2mz^2} + B \int_{-1}^1 d\beta \frac{m\gamma^3}{2m\gamma^3} \frac{f(E)}{(z - \beta)^2} H(\beta) \right] \\
 &= 16\pi\alpha n_0 \left[ \frac{1}{2mz^2} + \frac{B}{2} \int_{-1}^1 d\beta \frac{f(E)}{(\beta - z)^2} H(\beta) \right] \\
 &= 16\pi\alpha n_0 \left[ \frac{1}{2mz^2} + \frac{B}{2} \frac{\partial}{\partial z} \int_{-1}^1 d\beta \frac{f(E)}{\beta - z} H(\beta) \right].
 \end{aligned} \tag{7.4}$$

The last calculation in the previous equation introduces the derivative with respect to  $z$  in order to remove the double pole at  $\beta = z$ . The reasons for this will become clear. The difficulty now lies in calculating the last integral. The function  $f(E)$  is only numerical data from a simulation which cannot be integrated analytically. Therefore the function is approximated by analytical functions. How this is done will be discussed later in this chapter. The form  $f(E)$  is found to be

$$\begin{aligned}
 f(E) &= H(E - a)b(E - a)H(c - E) + H(E - c)dH(f - E) \\
 &\quad + H(E - f)de^{-g(E-f)}H(h - E)
 \end{aligned} \tag{7.5}$$

where  $a, b, c, d, f, g, h$  are all variational parameters determined by the simulated data. The last integral, which will be called  $I(z)$ , can then be split into three parts

$$\begin{aligned}
 I(z) &= \int_{-1}^1 d\beta H(m\gamma - a) \frac{b(m\gamma - a)}{\beta - z} H(c - m\gamma) H(\beta) \\
 &\quad + \int_{-1}^1 d\beta H(m\gamma - c) \frac{d}{\beta - z} H(f - m\gamma) H(\beta) \\
 &\quad + \int_{-1}^1 d\beta H(m\gamma - f) d \frac{e^{-g(m\gamma-f)}}{\beta - z} H(h - m\gamma) H(\beta).
 \end{aligned} \tag{7.6}$$

All terms has a pole at  $\beta = z$ . This means that the integrals can be split up into a real and imaginary part. To do this we use Plemelj's formula

$$\frac{1}{x - a + 0i} = \mathcal{P} \left( \frac{1}{x - a} \right) - i\pi\delta(x - a), \tag{7.7}$$

where  $\mathcal{P}$  denotes the principal value. Here lies the reason as to why the degree of the pole was reduced by introducing the derivative with respect to  $z$ . Plemelj's formula



only works with first order poles. With the pole rewritten with Plemelj's formula the integral takes the form of

$$\begin{aligned}
 I(z) &= \mathcal{P} \int_{-1}^1 d\beta H(m\gamma - a) \frac{b(m\gamma - a)}{\beta - z} H(c - m\gamma) H(\beta) \\
 &+ \mathcal{P} \int_{-1}^1 d\beta H(m\gamma - c) \frac{d}{\beta - z} H(f - m\gamma) H(\beta) + \int_{-1}^1 d\beta H(m\gamma - f) d \frac{e^{-g(m\gamma - f)}}{\beta - z} H(\beta) \\
 &- i\pi \left[ \int_{-1}^1 d\beta H(m\gamma - a) b(m\gamma - a) H(c - m\gamma) \delta(\beta - z) H(\beta) \right. \\
 &+ \left. \int_{-1}^1 d\beta H(m\gamma - c) d H(f - m\gamma) \delta(\beta - z) H(\beta) \right] H(1 - z) \\
 &= \mathcal{P} \int_0^1 d\beta H(m\gamma - a) \frac{b(m\gamma - a)}{\beta - z} H(c - m\gamma) + \mathcal{P} \int_0^1 d\beta H(m\gamma - c) \frac{d}{\beta - z} H(f - m\gamma) \\
 &+ \int_0^1 d\beta H(m\gamma - f) d \frac{e^{-g(m\gamma - f)}}{\beta - z} - i\pi [H(m\gamma_0 - a) b(m\gamma_0 - a) H(c - m\gamma_0) \\
 &H(m\gamma_0 - c) d H(f - m\gamma_0)] H(1 - z).
 \end{aligned} \tag{7.8}$$

The integral over the exponential function is not written out using Plemelj's formula because it is on the same form as the relativistic plasma dispersion function and will be calculated using the same method. The step function,  $H(1 - z)$ , appears because  $-1 < \beta < 1$  and there is only a pole for  $z < 1$ .

The two principal value integrals can be calculated explicitly. Beginning with the first, we use the known integral

$$\int \frac{dx}{(x - a)\sqrt{1 - x^2}} = \begin{cases} \frac{-1}{\sqrt{1 - a^2}} \ln \left[ C_1 \frac{1 - ax + \sqrt{(1 - a^2)(1 - x^2)}}{x - a} \right] & \text{for } a < 1 \\ \frac{1}{\sqrt{a^2 - 1}} \arcsin \frac{1 - ax}{|x - a|} + C_2 & \text{for } a > 1 \\ -\sqrt{\frac{1 + x}{1 - x}} + C_3 & \text{for } a = 1 \end{cases}. \tag{7.9}$$

With this the part of our integral that is linear in  $E$  becomes, for  $z < 1$ ,

$$\begin{aligned}
 &\mathcal{P} \int_0^1 H(m\gamma - a) \frac{bm\gamma}{\beta - z} H(m\gamma - c) \\
 &= bm \left[ \int_{\beta_1}^{z - \epsilon} \frac{d\beta}{(\beta - z)\sqrt{1 - \beta^2}} + \int_{z + \epsilon}^{\beta_2} \frac{d\beta}{(\beta - z)\sqrt{1 - \beta^2}} \right] \\
 &= \frac{-bm}{\sqrt{1 - z^2}} \ln \left( \frac{1 - z\beta_2 + \sqrt{(1 - z^2)(1 - \beta_2^2)}}{1 - z\beta_1 + \sqrt{(1 - z^2)(1 - \beta_1^2)}} \right).
 \end{aligned} \tag{7.10}$$

$\beta_1$  and  $\beta_2$  are defined to satisfy the step functions, that is  $m(1 - \beta_1^2)^{-1/2} = a$  and  $m(1 - \beta_2^2)^{-1/2} = c$ . For  $z > 1$  it is

$$\begin{aligned}
 &\int_0^1 d\beta H(m\gamma - a) \frac{bm\gamma}{\beta - z} H(m\gamma - c) = \int_{\beta_1}^{\beta_2} d\beta \frac{bm}{(\beta - z)\sqrt{1 - \beta^2}} \\
 &= \frac{bm}{\sqrt{z^2 - 1}} \left[ \arcsin \left( \frac{1 - z\beta_2}{z - \beta_2} \right) - \arcsin \left( \frac{1 - z\beta_1}{z - \beta_1} \right) \right].
 \end{aligned} \tag{7.11}$$

The absolute value has been dropped since  $-1 < \beta < 1$  which makes  $\beta - z$  always negative when  $z > 1$ . The two constant functions are integrated as follows

$$\begin{aligned} \mathcal{P} \int_0^1 d\beta H(m\gamma - a) \frac{-ba}{\beta - z} H(c - m\gamma) &= \int_{\beta_1}^{z-\epsilon} d\beta \frac{-ba}{\beta - z} + \int_{z+\epsilon}^{\beta_2} d\beta \frac{-ba}{\beta - z} \\ &= -ba \ln \left| \frac{\beta_2 - z}{\beta_1 - z} \right|, \end{aligned} \quad (7.12)$$

and similarly for

$$\mathcal{P} \int_0^1 d\beta H(m\gamma - c) \frac{d}{\beta - z} H(f - m\gamma) = d \ln \left| \frac{\alpha_2 - z}{\alpha_1 - z} \right|, \quad (7.13)$$

where  $m(1 - \alpha_1^2)^{-1/2} = c$  and  $m(1 - \alpha_2^2)^{-1/2} = f$ . The last integral is on the same form as the RPDF except for the extra step functions. The step functions make it so the integrand no longer becomes modified Bessel functions. Instead the integrand looks like

$$Q_\nu(x) = \frac{(x/2)^\nu \Gamma(\frac{1}{2})}{\Gamma(\nu + \frac{1}{2})} \int_{\chi_1}^{\chi_2} d\chi \sinh \chi^{2\nu} e^{-x \cosh \chi}, \quad (7.14)$$

which is exactly the same as the integral definition of the MacDonald function, see appendix A, except for the integration limits. The limits are defined as  $\chi_1 = \cosh^{-1}(f/m)$  and  $\chi_2 = \cosh^{-1}(h/m)$ . In analogue with the RPDF the integral over the exponential function can be rewritten as

$$\begin{aligned} &\int_0^1 d\beta H(m\gamma - f) C \frac{e^{-g(m\gamma - f)}}{\beta - z} H(h - m\gamma) \\ &= \begin{cases} -d \frac{2gm}{1-z^2} e^{gf} \int_0^z d\zeta \frac{Q_1(mgR)}{R} + i\pi e^{-g(m\gamma_0 - f)} & \text{for } z < 1 \\ d \frac{2gm}{1-z^2} e^{gf} \int_z^\infty d\zeta \frac{Q_1(mgR)}{R} & \text{for } z > 1 \end{cases}. \end{aligned} \quad (7.15)$$

The combined expression for  $I(z)$  is, for  $z < 1$ ,

$$\begin{aligned} I(z) &= -\frac{bm}{\sqrt{1-z^2}} \ln \left( \frac{1 - z\beta_2 + \sqrt{(1-z^2)(1-\beta_2^2)}}{1 - z\beta_1 + \sqrt{(1-z^2)(1-\beta_1^2)}} \right) + d \ln \left| \frac{\alpha_2 - z}{\alpha_1 - z} \right| - ba \ln \left| \frac{\beta_2 - z}{\beta_1 - z} \right| \\ &\quad - d \frac{2gm}{1-z^2} e^{gf} \int_0^z d\zeta \frac{Q_1(mgR)}{R} - i\pi [H(m\gamma_0 - a)b(m\gamma_0 - a)H(c - m\gamma_0) \\ &\quad + H(m\gamma_0 - c)dH(f - m\gamma_0) - H(m\gamma_0 - f)de^{-g(m\gamma - f)}H(h - m\gamma_0)]. \end{aligned} \quad (7.16)$$

For  $z > 1$  it is

$$\begin{aligned} I(z) &= \frac{bm}{\sqrt{z^2 - 1}} \left[ \arcsin \left( \frac{1 - z\beta_2}{z - \beta_2} \right) - \arcsin \left( \frac{1 - z\beta_1}{z - \beta_1} \right) \right] \\ &\quad + d \ln \left| \frac{\alpha_2 - z}{\alpha_1 - z} \right| - ba \ln \left| \frac{\beta_2 - z}{\beta_1 - z} \right| + d \frac{2gm}{1-z^2} e^{gf} \int_z^\infty d\zeta \frac{Q_1(mgR)}{R}. \end{aligned} \quad (7.17)$$

The total expression for the 00-component of the response tensor is, using  $\alpha = q^2/4\pi$ ,

$$\Pi^{00} = 4q^2 n_0 \left[ \frac{1}{2mz^2} + \frac{B}{2} \frac{\partial}{\partial z} I(z) \right]. \quad (7.18)$$

To calculate the absorption coefficient we need the derivative of  $\text{Re}\Pi^{00}$  with respect to  $\omega$

$$\begin{aligned}
 \frac{\partial}{\partial\omega}\text{Re}\Pi^{00} &= \frac{1}{|\mathbf{k}|} \frac{\partial}{\partial z} \text{Re}\Pi^{00} \\
 &= \frac{4q^2 n_0}{|\mathbf{k}|} \frac{\partial}{\partial z} \left[ \frac{1}{2mz^2} + \frac{B}{2} \frac{\partial}{\partial z} \text{Re}I(z) \right] \\
 &= \frac{4q^2 n_0}{|\mathbf{k}|} \left[ -\frac{1}{mz^3} + \frac{B}{2} \frac{\partial^2}{\partial z^2} \text{Re}I(z) \right].
 \end{aligned} \tag{7.19}$$

The next step is to find the normalizing factor  $R_L$  defined in equation (4.25). We find the derivative of  $\Lambda_L$ , remembering that  $\Lambda_L = k^2(e_L \cdot e_L) - (k \cdot e_L)(k \cdot e_L) + \mu_0 \text{Re}\Pi_L$  and  $\Pi_L = (1 - z^2)^{-1}$ ,

$$\begin{aligned}
 \frac{\partial}{\partial\omega}\Lambda_L &= -2\omega + \mu_0 \frac{\partial}{\partial\omega} \text{Re}\Pi_L \\
 &= -2\omega + \mu_0 \frac{\partial}{\partial z} \left[ (1 - z^2)^{-1} 4q^2 n_0 \left( \frac{1}{2mz^2} + \frac{B}{2} \frac{\partial}{\partial z} \text{Re}I(z) \right) \right] \\
 &= -2\omega + \frac{4q^2 \mu_0 n_0}{|\mathbf{k}|} \left[ \frac{2z}{(1 - z^2)^2} \left( \frac{1}{2mz^2} + \frac{B}{2} \frac{\partial}{\partial z} \text{Re}I(z) \right) \right. \\
 &\quad \left. + \frac{1}{1 - z^2} \left( -\frac{1}{mz^3} + \frac{B}{2} \frac{\partial^2}{\partial z^2} \text{Re}I(z) \right) \right].
 \end{aligned} \tag{7.20}$$

Put into (6.14)  $R_L^{-1}$  becomes

$$\begin{aligned}
 R_L^{-1} &= 2 - \frac{4q^2 \mu_0 n_0 z}{\omega_L} \left[ \frac{2z}{(1 - z^2)^2} \left( \frac{1}{2mz^2} + \frac{B}{2} \frac{\partial}{\partial z} \text{Re}I(z) \right) \right] \\
 &\quad + \frac{1}{1 - z^2} \left( -\frac{1}{mz^3} + \frac{B}{2} \frac{\partial^2}{\partial z^2} \text{Re}I(z) \right) \\
 &= 2 - \frac{4q^2 \mu_0 n_0 z}{\omega_L (1 - z^2)} \left[ \frac{2z}{1 - z^2} \left( \frac{1}{2mz^2} + \frac{B}{2} \frac{\partial}{\partial z} \text{Re}I(z) \right) \right. \\
 &\quad \left. + \left( -\frac{1}{mz^2} + \frac{B}{2} \frac{\partial^2}{\partial z^2} \text{Re}I(z) \right) \right].
 \end{aligned} \tag{7.21}$$

We also need the anti-hermitian part of  $\Pi_L$ . It is

$$\Pi_L^A = (1 - z^2)^{-1} i \text{Im}\Pi^{00} = \frac{4iq^2 n_0 B}{2(1 - z^2)} \frac{\partial}{\partial z} \text{Im}I(z). \tag{7.22}$$

With all the components the absorption coefficient is

$$\begin{aligned}
 \gamma_L &= 2i \frac{R_L}{\epsilon_0 \omega_L} \Pi_L^A \\
 &= -\frac{4q^2 n_0 B}{\epsilon \omega_L} \frac{\partial}{\partial z} \text{Im}I(z) \\
 &\times \left\{ 2 - \frac{4q^2 \mu_0 n_0 z}{\omega_L^2 (1-z^2)} \left[ \frac{2z}{1-z^2} \left( \frac{1}{2mz^2} + \frac{B}{2} \frac{\partial}{\partial z} \text{Re}I(z) \right) - \frac{1}{mz^3} + \frac{B}{2} \frac{\partial^2}{\partial z^2} \text{Re}I(z) \right] \right\}^{-1} \\
 &= -\frac{4mB\omega_{p,0}^2}{\omega_L(1-z^2)} \frac{\partial}{\partial z} \text{Im}I(z) \\
 &\times \left\{ 2 - \frac{4\omega_{p,0}^2 z}{\omega_L^2 (1-z^2)} \left[ \frac{2z}{1-z^2} \left( \frac{1}{2z^2} + \frac{Bm}{2} \frac{\partial}{\partial z} \text{Re}I(z) \right) - \frac{1}{z^3} + \frac{Bm}{2} \frac{\partial^2}{\partial z^2} \text{Re}I(z) \right] \right\}^{-1}.
 \end{aligned} \tag{7.23}$$

The plasma frequency has again been introduced as  $\omega_{p,0}^2 = \frac{q^2 n_0}{\epsilon_0 m}$  which is the same as earlier just with  $n_0$  instead of  $n$ . The derivatives of  $I(z)$  is written in Appendix B.

There are also three variables in this new expression; they are the phase velocity  $z$ , the density ratio  $B \equiv r \cdot n_b/n_0$  and the ratio of the plasma frequency and the frequency in the wave mode  $x_0 \equiv \omega_{p,0}/\omega_L$ . The values of  $n_b$  and  $n_0$  is  $10^{-22} \text{ m}^{-3}$  and  $10^{-7} \text{ m}^{-3}$  respectively [1].  $r$  is used as a free variable tuning the density ratio. This absorption coefficient is inherently ultrarelativistic because of the high energy of the simulated data. This leads to a problem where the absorption coefficient is only non-zero when the phase velocity is 99.999999% of the speed of light making it numerically difficult to consider. In order to make this simpler we increase the mass until it is very close to the value of  $a$ , see equation (7.27), effectively lowering the energy of the particles in the beam. The absorption coefficient is plotted for three different values of  $r$ . Namely  $r = 0.01$  in Figure 7.1,  $r = 1$  in Figure 7.2 and  $r = 100$  in Figure 7.3 with  $x_0 = 165$ .

As with the absorption coefficient for the Jüttner distribution the divergence is caused by  $R_L$  becoming zero. The absorption coefficient is also only negative when  $R_L$  is because  $\Pi_L$  with prefactors is positive. This can be seen from

$$-\frac{4mB\omega_{p,0}^2}{\omega_L(1-z^2)} \frac{\partial}{\partial z} \text{Im}I(z). \tag{7.24}$$

The prefactors are negative and so is  $\frac{\partial}{\partial z} \text{Im}I(z)$ , see appendix B, making the total expression positive. This is illustrated in figure 7.4 which shows  $\Pi_L$  with prefactors and  $R_L$  as a function of  $z$  separately for  $r = 1$  and  $x_0 = 165$ . Here as well one can set a criteria for an instability. It is again that  $R_L \leq 0$ , or

$$2 \leq \frac{4\omega_{p,0}^2 z}{\omega_L^2 (1-z^2)} \left[ \frac{2z}{1-z^2} \left( \frac{1}{2z^2} + \frac{Bm}{2} \frac{\partial}{\partial z} \text{Re}I(z) \right) - \frac{1}{z^3} + \frac{Bm}{2} \frac{\partial^2}{\partial z^2} \text{Re}I(z) \right]. \tag{7.25}$$

The absorption coefficient has the same issues as the one with the Jüttner distribution. It diverges to plus/minus infinity at certain values of  $z$ ,  $B$  and  $x$ . As said in the previous chapter this is unphysical and there is an inconsistency in the calculations as before. This makes sense as Plemelj's formula has been employed in this calculation as well.

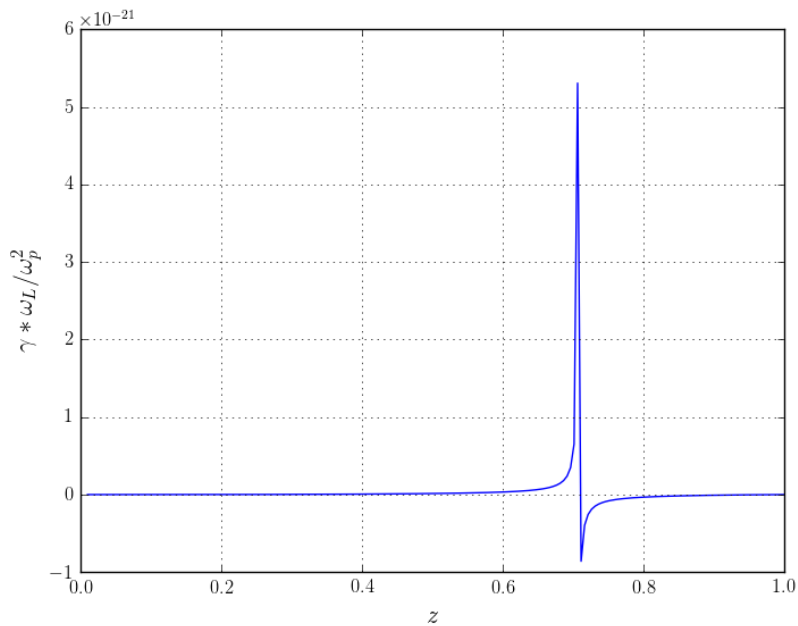


Figure 7.1: The figure shows the absorption coefficient as a function of  $z$  for  $r = 0.01$  and  $x_0 = 165$ . It is positive, stable, until it diverges and after the divergence it is negative, unstable.

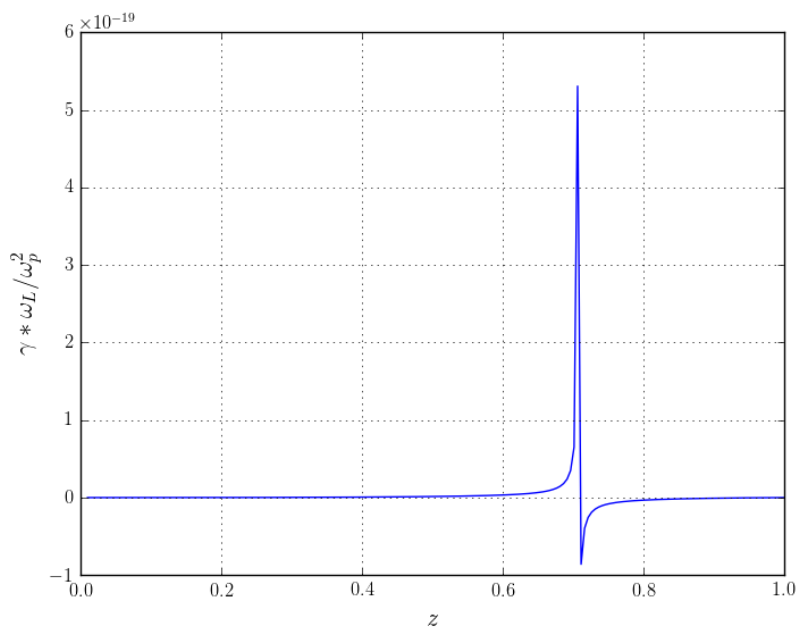


Figure 7.2: The figure shows the absorption coefficient as a function of  $z$  for  $r = 1$  and  $x_0 = 165$ . It is positive, stable, until it diverges and after the divergence it is negative, unstable.

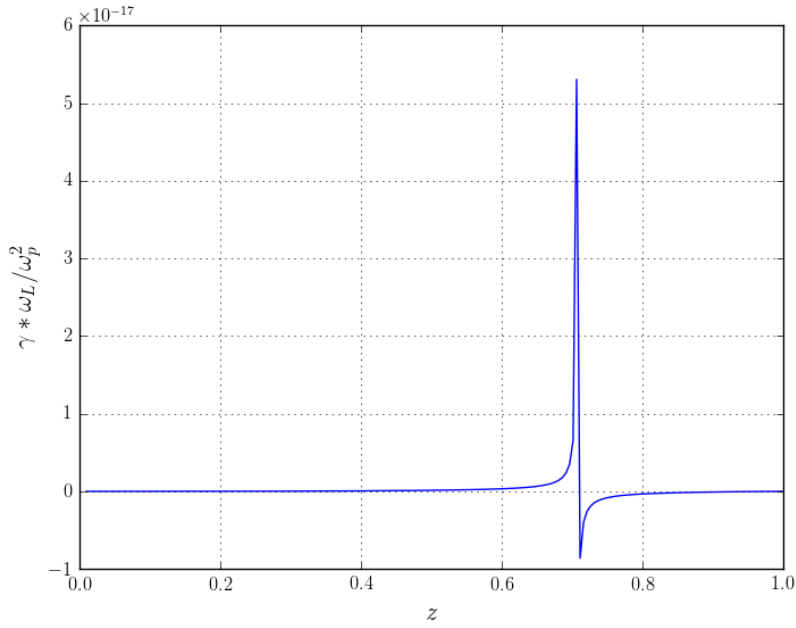


Figure 7.3: The figure shows the absorption coefficient as a function of  $z$  for  $r = 100$  and  $x_0 = 165$ . It is positive, stable, until it diverges and after the divergence it is negative, unstable.

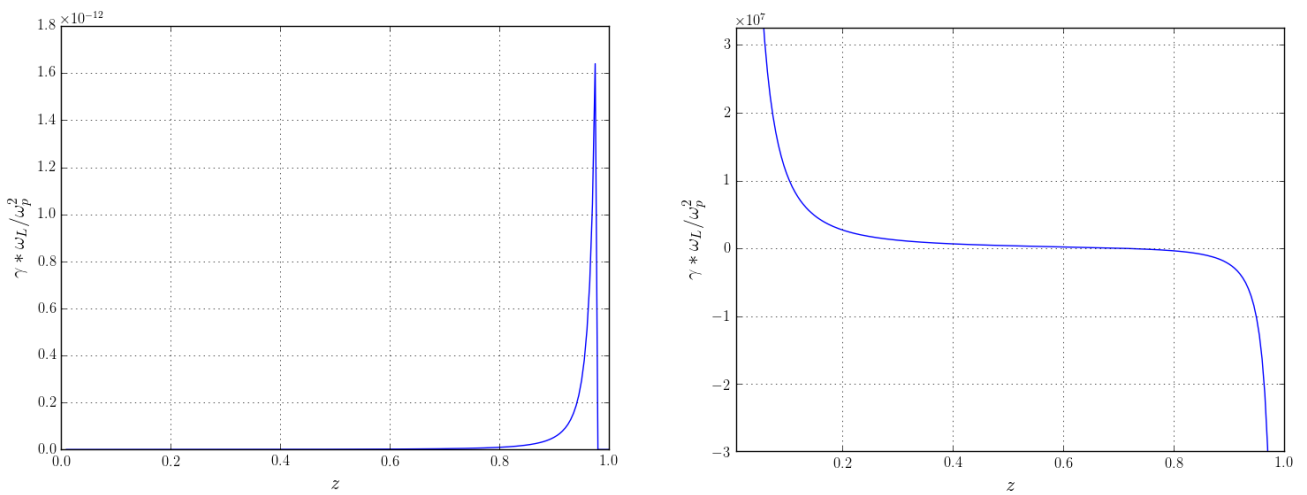


Figure 7.4: The figure shows  $\Pi_L$  with prefactors (left) and  $R_L$  (right) as a function of  $z$  for  $r = 1$  and  $x_0 = 165$ . One can see that  $\Pi_L$  with prefactors is positive while  $R_L$  is both positive and negative.

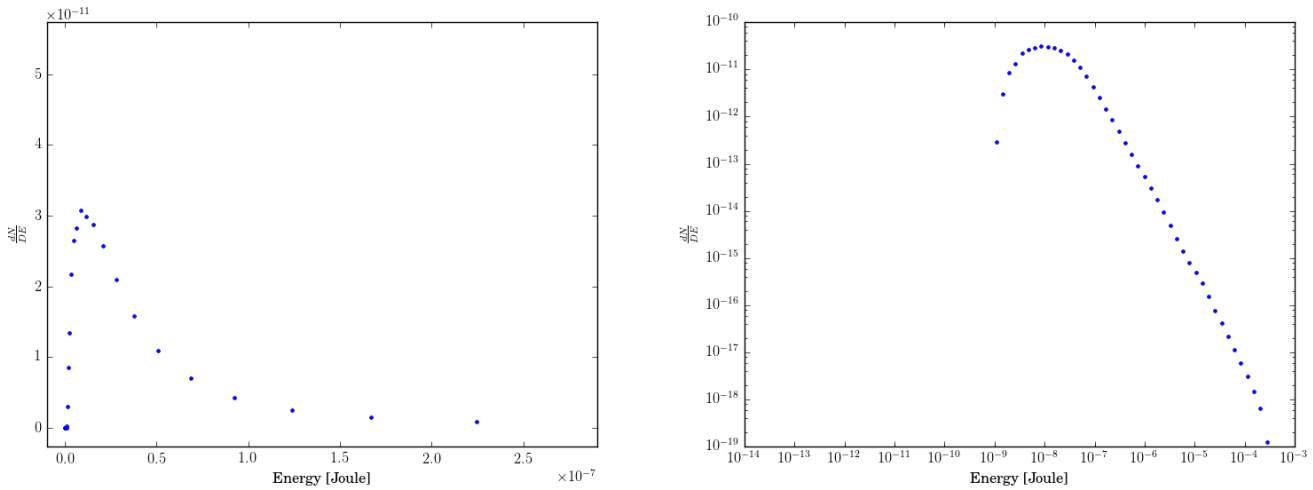


Figure 7.5: Plots of the data points from the simulations using ELMAG [22]. It shows the spectrum of the first generation of  $e^+e^-$  pairs in an electromagnetic cascade on the extragalactic background light. The left graph is plotted with logarithmic axis and the right graph is plotted with linear axis. Note that some data points are missing in each graph. The logarithmic graph are missing the data points which have a zero value on the y-axis. The linear graph is missing some data points at the high energy.

## 7.2 The Distribution Function

The distribution function used in the foregoing calculation is

$$n(E) = n_0(2\pi)^3 \delta(p_x) \delta(p_y) [\delta(p_z) + B f(E) H(\beta)]. \quad (7.26)$$

This distribution function defines a beam of particles travelling in the  $z$ -direction in a background of particles. The momentum in  $x$ - and  $y$ -direction is put to zero by the delta functions. The background particles are related to the first term. It is stationary and therefore has a delta function over  $p_z$ . The last term is related to the particle beam. The constant  $B$  is the ratio of the beam density and the background density,  $B = r \frac{n}{n_0}$ . The step function with the argument  $\beta$  expresses that the particles in the beam only move in one direction, away from the source. The function  $f(E) = \frac{dN}{dE}$  is the distribution of particles over energy. The distribution is found using ELMAG [22]. Here, ELMAG is used to simulate the spectrum of the first generation of  $e^+e^-$  pairs in the electromagnetic cascade on the extragalactic background light. The data points are shown in Figure 7.5 both with linear and logarithmic axis. The energy units are in joule. Performing an analytical integration over this function is necessary because the result of the integration has to be differentiated twice which would lead to unacceptable error. In order to do it analytically we need to fit an analytic function to the data points. To do this the data points were split into three regions. The central flat part and two tails. The leftmost tail was approximated by a linear function  $y_1 = b(E - a)$  with a gradient  $b$  starting at energy  $a$  and ending at  $c$ . The central part is approximated by a constant with a value of  $y_2 = d$  starting at  $c$  and ending at  $f$ .  $d$  is not a free variable as it is defined by  $b$ ,  $a$  and  $c$  with the requirement that  $f(E)$  is continuous. The rightmost tail is approximated by a

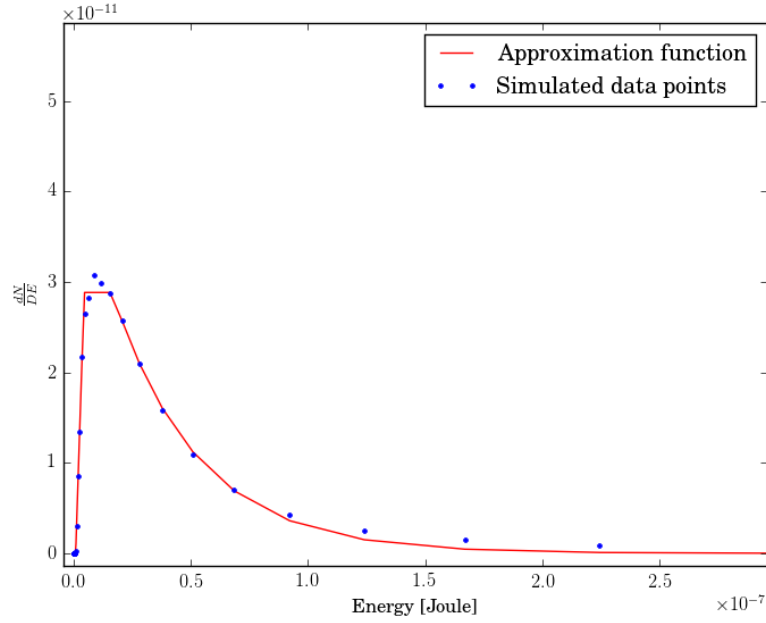


Figure 7.6: The figure shows the simulated data points of the distribution of particles over energy with the approximation function giving an analytic expression for it.

decaying exponential function  $y_3 = de^{-g(E-f)}$  starting at  $f$  and ending at  $h$ . The values of the constants  $a, b, c, d, f, g, h$  are found numerically by minimizing the mean square error of the distance between the data points and  $f(E)$ . The values are

$$\begin{aligned}
 a &= 0.9566 \cdot 10^{-9} \text{ Joule} \\
 b &= 7.9038 \cdot 10^{16} \text{ 1/Joule} \\
 c &= 4.5950 \cdot 10^{-9} \text{ Joule} \\
 d &= 2.8836 \cdot 10^{-11} \text{ 1/Joule} \\
 f &= 1.6587 \cdot 10^3 \text{ Joule} \\
 g &= 2.7497 \cdot 10^{-6} \text{ 1/Joule} \\
 h &= 2.6500 \cdot 10^5 \text{ Joule.}
 \end{aligned}
 \tag{7.27}$$

The function  $f(E)$  with these values is plotted with the data points in Figure 7.6.



## 8 — Summary and Conclusion

The goal of this thesis was to find the growth rate of plasma instabilities in an electron-positron plasma beam and then compare the time scale of this growth rate to that of the inverse Compton cascade to see if it could be a competing energy loss mechanism. If it was, plasma instability could be used to explain the non-detection of an electromagnetic cascade in beams from blazars avoiding the introduction of an intergalactic magnetic field. This thesis would then support or contradict the work done by Supsar [1] and Schlikeiser et. al. [2, 3], which concluded that the non-detection of the electromagnetic cascade could indeed be explained by plasma instabilities.

We employed a covariant formalism of plasma theory following Ref [14]. Using this theory we derived the linear response tensor for a plasma with particles distributed according to the Jüttner distribution and used this to find an expression for the absorption coefficient of the plasma. In addition this first part also introduced an alternative expression for LRT which lead to a similar expression for the absorption coefficient.

In the next part of the thesis we recalculated the absorption coefficient for a new distribution of particles. This new distribution was based on a simulation of the electromagnetic cascade and had to be approximated by an analytic function numerically.

We wanted to find the minimum (most negative) value of these two absorption coefficients and compare their corresponding time scale to that of the inverse Compton cascade, but this turned out not to be possible. The absorption coefficient diverged and became formally minus infinity, in both cases, for certain values of the phase velocity, the relativistic factor  $m/T$  and the ratio  $\omega_p/\omega_L$ , which is not physical, forcing us to conclude that there were problems with some part of the calculation. This problem most likely occurs when Plemelj's formula is used to split the LRT into a real and imaginary part. To do this we assume that the imaginary absorption coefficient is small, which was found to not be a self-consistent assumption due to the divergences. Because of this problem with the calculation we could draw no conclusions which supported or opposed the work done by Supsar and Schlikeiser et. al.

In order to find the maximum value of the growth rate as was the goal of this thesis one would have to redo the calculations, this time avoiding the assumption that the growth rate is small. Another option could be to treat the infinities in such a way as to deduce the actual maximum values. It could be more sensible to do this process numerically using for instance the recently developed *Arbitrary Linear Plasma Solver* [23].



# A — MacDonald functions

Bessel functions are important mathematical functions which show up in several different branches of physics. For instance as the solutions of the radial Schrödinger equation, electromagnetic waves in a cylinder and several problems in signal processes. Bessel functions are defined as the solutions of the differential equation [24]

$$\frac{d^2}{dx^2}K_\nu(x) + \frac{1}{x} \frac{d}{dx}K_\nu(x) + \left(1 - \frac{\nu^2}{x^2}\right) K_\nu(x) = 0. \quad (\text{A.1})$$

$\nu$  can be any complex number, but integer values and half integer values are most important cases. This differential equation is of second order and has two linearly independent solutions. The Bessel functions of the first kind are the solutions which are finite at the origin, while the Bessel functions of the second kind are infinite at the origin. Both are shown in Figure A.1.

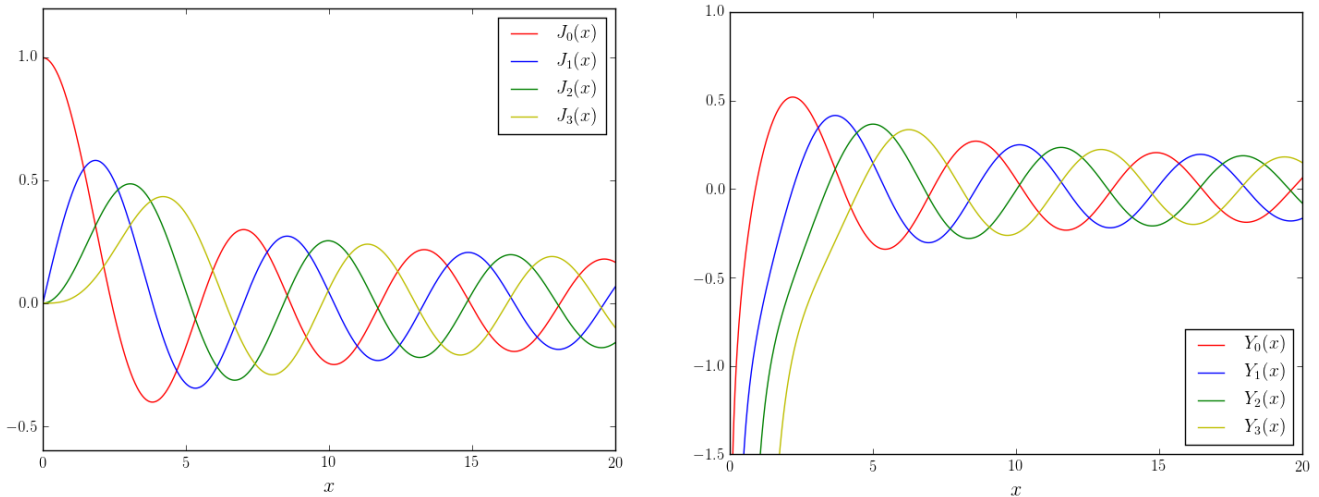


Figure A.1: The first 4 orders of the Bessel function of the first (right) and second (left) kind.

Modified Bessel functions are defined similarly to the Bessel functions. They are defined by the differential equation [24]

$$\frac{d^2}{dx^2}K_\nu(x) + \frac{1}{x} \frac{d}{dx}K_\nu(x) - \left(1 + \frac{\nu^2}{x^2}\right) K_\nu(x) = 0. \quad (\text{A.2})$$

The difference to the Bessel functions are the opposite sign on the constant term. The solutions which are infinite at the origin are the modified Bessel functions of

the second kind, also known as MacDonal functions, and can be seen in figure A.2. The MacDonal functions does not oscillate like the Bessel functions, but decay exponentially. All types of Bessel functions can be written as integrals. The integral

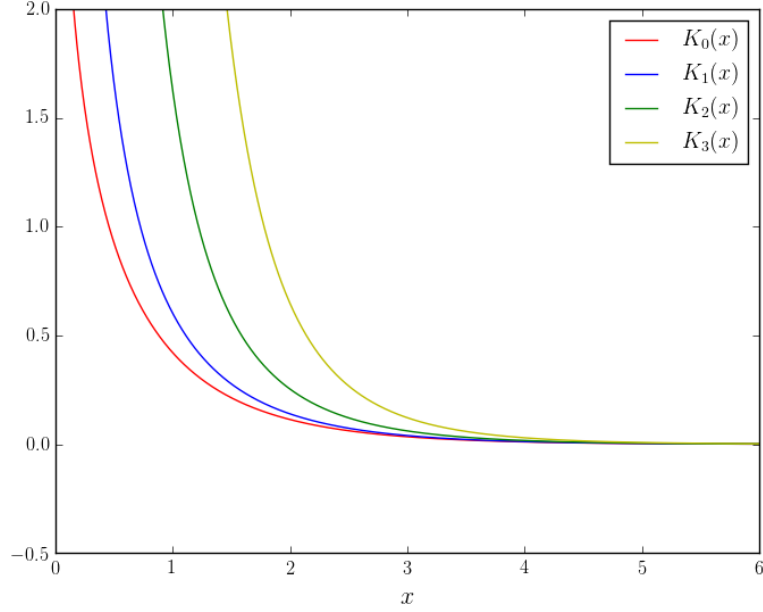


Figure A.2: The first 4 orders of the modified Bessel function of the second kind.

form of the MacDonal functions are [24]

$$K_\nu(x) = \frac{(x/2)^\nu \Gamma(\frac{1}{2})}{\Gamma(\nu + \frac{1}{2})} \int_0^\infty d\chi \sinh^{2\nu}(\chi) e^{-x \cosh(\chi)}. \quad (\text{A.3})$$

They also satisfy the recursion relations

$$\begin{aligned} K_{\nu-1}(x) - K_{\nu+1}(x) &= -2\frac{\nu}{x} K_\nu(x), \\ K_{\nu-1}(x) + K_{\nu+1}(x) &= -2\frac{d}{dx} K_\nu(x). \end{aligned} \quad (\text{A.4})$$

For small  $x$ , corresponds to ultrarelativistic speeds, the MacDonal functions can be expanded as

$$K_\nu \approx \frac{2^{\nu-1}(\nu-1)!}{x^\nu} \quad (\text{A.5})$$

and for large  $x$ , corresponding to classical speeds, as

$$K_\nu(x) = \left(\frac{\pi}{2x}\right)^2 e^{-x} \left(1 + \frac{4\nu^2 - 1}{8x} + \frac{(4\nu^2 - 1)(4\nu^2 - 9)}{128x^2} + \dots\right). \quad (\text{A.6})$$

## B — Derivatives

The derivatives necessary to calculate the absorption coefficient both for the Jüttner distribution (6.16) and the simulated distribution (7.23) are included in this appendix.

### B.1 Derivatives of the Relativistic Particle Distribution Function

The derivatives of the RPDF with respect to  $\rho$  and  $z$  present in 6.16 are calculated here. They are done using the rule

$$\frac{d}{dt} \int_0^t dx g(x, t) = \int_0^t dx \frac{\partial g(x, t)}{\partial t} + g(t, t). \quad (\text{B.1})$$

The double derivative with respect to  $\rho$  is

$$\frac{\partial^2 T(z, \rho)}{\partial \rho^2} = \begin{cases} -\frac{2}{1-z^2} \left[ \rho \int_0^z d\zeta R K_1''(\rho R) + 2 \int_0^z d\zeta K_1'(\rho R) \right] + i\pi \gamma_0^2 e^{-\rho \gamma_0} & \text{for } z < 1 \\ \frac{2}{1-z^2} \left[ \rho \int_z^\infty d\zeta R K_1''(\rho R) + 2 \int_z^\infty d\zeta K_1'(\rho R) \right] & \text{for } z > 1 \end{cases} \quad (\text{B.2})$$

An additional derivative with respect to  $z$  is, now divided into  $z < 1$

$$\begin{aligned} \frac{\partial^2 T'(z, \rho)}{\partial \rho^2} = & -\frac{2}{1-z^2} \left[ \frac{z}{1-z^2} \int_0^z d\zeta (2K_1'(\rho R) + 4\rho R K_1''(\rho R) + \rho^2 R^2 K_1^{(3)}(\rho R)) \right. \\ & \left. + 2K_1'(\rho) + \rho K_1''(\rho) \right] + i\pi z \gamma_0^4 (2 - \rho \gamma_0) e^{-\rho \gamma_0}, \end{aligned} \quad (\text{B.3})$$

and  $z > 1$

$$\begin{aligned} \frac{\partial^2 T'(z, \rho)}{\partial \rho^2} = & \frac{2}{1-z^2} \left[ \frac{z}{1-z^2} \int_z^\infty d\zeta (2K_1'(\rho R) + 4\rho R K_1''(\rho R) + \rho^2 R^2 K_1^{(3)}(\rho R)) \right. \\ & \left. - 2K_1'(\rho) - \rho K_1''(\rho) \right]. \end{aligned} \quad (\text{B.4})$$

Another derivative with respect to  $z$  gives

$$\begin{aligned} \frac{\partial T''(z, \rho)}{\partial \rho^2} = & -\frac{2}{1-z^2} \left\{ \frac{1}{1-z^2} \int_0^z d\zeta \left[ 2K_1'(\rho R) + 4\rho R K_1''(\rho R) + \rho^2 R^2 K_1^{(3)}(\rho R) \right. \right. \\ & \left. \left. + z^2(6K_1'(\rho R) + 18\rho R K_1''(\rho R) + 8\rho^2 R^2 K_1^{(3)}(\rho R) + \rho^3 R^3 K_1^{(4)}(\rho R)) \right] \right. \\ & \left. + z(6K_1'(\rho) + 6\rho K_1''(\rho) + \rho^2 K_1^{(3)}(\rho)) \right\} + i\pi z^2 \gamma_0^6 (2 - 4\rho\gamma_0 + \rho^2 \gamma_0^2) e^{-\rho\gamma_0}, \end{aligned} \quad (\text{B.5})$$

for  $z < 1$  and

$$\begin{aligned} \frac{\partial T''(z, \rho)}{\partial \rho^2} = & \frac{2}{1-z^2} \left\{ \frac{1}{1-z^2} \int_z^\infty d\zeta \left[ 2K_1'(\rho R) + 4\rho R K_1''(\rho R) + \rho^2 R^2 K_1^{(3)}(\rho R) \right. \right. \\ & \left. \left. + z^2(6K_1'(\rho R) + 18\rho R K_1''(\rho R) + 8\rho^2 R^2 K_1^{(3)}(\rho R) + \rho^3 R^3 K_1^{(4)}(\rho R)) \right] \right. \\ & \left. - z(6K_1'(\rho) + 6\rho K_1''(\rho) + \rho^2 K_1^{(3)}(\rho)) \right\} \end{aligned} \quad (\text{B.6})$$

for  $z > 1$ . The prime signifies the derivative with respect to  $z$  when used with the RPDF and the derivative with respect to its argument when used with the MacDonalld functions.

## B.2 Derivatives of $I(z)$ for $z < 1$

The first and second derivatives of  $I(z)$  is a part of the absorption coefficient (7.23) for the simulated distribution and are shown here. They are split into this section for  $z < 1$  and the next section for  $z > 1$  and the different terms are done separately to make the expression a bit shorter. Some of the calculations are done by hand and some of them are done using digital tools. All the calculations use only basic derivative rules.

Let us first look at

$$\ln \left| \frac{\alpha_2 - z}{\alpha_1 - z} \right|. \quad (\text{B.7})$$

We split it into to parts to remove the absolute values. First for  $\alpha_1 < z < \alpha_2$  the derivative is

$$\begin{aligned} \frac{\partial}{\partial z} \ln \left( \frac{\alpha_2 - z}{z - \alpha_1} \right) &= \frac{z - \alpha_1}{\alpha_2 - z} \left( \frac{-1}{z - \alpha_1} - \frac{\alpha_2 - z}{(z - \alpha_1)^2} \right) \\ &= \frac{z - \alpha_1}{\alpha_2 - z} \left( \frac{\alpha_1 - z - \alpha_2 + z}{(z - \alpha_1)^2} \right) = \frac{(z - \alpha_1)(\alpha_1 - \alpha_2)}{(\alpha_2 - z)(z - \alpha_1)^2} \\ &= \frac{\alpha_1 - \alpha_2}{(\alpha_2 - z)(z - \alpha_1)}. \end{aligned} \quad (\text{B.8})$$

For  $z < \alpha_1 \vee z > \alpha_2$  it is

$$\frac{\partial}{\partial z} \ln \left( \frac{\alpha_2 - z}{\alpha_1 - z} \right) = \frac{\alpha_1 - \alpha_2}{(\alpha_1 - z)(z - \alpha_2)} = \frac{\alpha_1 - \alpha_2}{(z - \alpha_1)(\alpha_2 - z)}. \quad (\text{B.9})$$

The results are the same so the result is the same for all values of  $z$ . The double derivative is

$$\frac{\partial^2}{\partial z^2} \ln \left| \frac{\alpha_2 - z}{\alpha_1 - z} \right| = \frac{(\alpha_1 - \alpha_2)(\alpha_1 + \alpha_2 - 2z)}{(z - \alpha_1)^2(\alpha_2 - z)^2}. \quad (\text{B.10})$$

One other term in  $I(z)$  is exactly the same, but with  $\beta$  instead of  $\alpha$  and its derivative is ofcourse the same. The other logarithmic term

$$\frac{1}{\sqrt{1-z^2}} \ln \left( \frac{1 - z\beta_2 + \sqrt{(1-z^2)(1-\beta_2^2)}}{1 - z\beta_1 + \sqrt{(1-z^2)(1-\beta_1^2)}} \right) \quad (\text{B.11})$$

is a bit more complicated and its derivatives are calculated by digital tools for convenience. The first derivative with respect to  $z$  is

$$\begin{aligned} & \frac{\partial}{\partial z} \frac{1}{\sqrt{1-z^2}} \ln \left( \frac{1 - z\beta_2 + \sqrt{(1-z^2)(1-\beta_2^2)}}{1 - z\beta_1 + \sqrt{(1-z^2)(1-\beta_1^2)}} \right) \\ &= - \frac{bm \ln \left( \frac{1-z\beta_2 + \sqrt{(1-z^2)(1-\beta_2^2)}}{1-z\beta_1 + \sqrt{(1-z^2)(1-\beta_1^2)}} \right) z}{(1-z^2)^{3/2}} \\ & - \frac{bm(1 - z\beta_1 + \sqrt{(1-z^2)(1-\beta_1^2)})}{\sqrt{1-z^2}(1 - z\beta_2 + \sqrt{(1-z^2)(1-\beta_2^2)})} \left[ \frac{-\beta_2 - \frac{z(1-\beta_2^2)}{\sqrt{(1-z^2)(1-\beta_2^2)}}}{1 - z\beta_1 + \sqrt{(1-z^2)(1-\beta_1^2)}} \right. \\ & \left. - \frac{(1 - z\beta_2 + \sqrt{(1-z^2)(1-\beta_2^2)}) \left( -\beta_1 - \frac{z(1-\beta_1^2)}{\sqrt{(1-z^2)(1-\beta_1^2)}} \right)}{(1 - z\beta_1 + \sqrt{(1-z^2)(1-\beta_1^2)})^2} \right], \end{aligned} \quad (\text{B.12})$$

and the second derivative is

$$\begin{aligned}
& \frac{\partial^2}{\partial z^2} \frac{1}{\sqrt{1-z^2}} \ln \left( \frac{1-z\beta_2 + \sqrt{(1-z^2)(1-\beta_2^2)}}{1-z\beta_1 + \sqrt{(1-z^2)(1-\beta_1^2)}} \right) \\
&= -\frac{bm}{\sqrt{1-z^2}} \left\{ 3 \frac{z^2}{(1-z^2)^2} \ln \left( \frac{1-z\beta_2 + \sqrt{(1-z^2)(1-\beta_2^2)}}{1-z\beta_1 + \sqrt{(1-z^2)(1-\beta_1^2)}} \right) \right. \\
&+ 2 \frac{(1-z\beta_1 + \sqrt{(1-z^2)(1-\beta_1^2)})z}{(1-z^2)(1-z\beta_2 + \sqrt{(1-z^2)(1-\beta_2^2)})} \\
&\times \left[ \frac{1}{1-z\beta_1 + \sqrt{(1-z^2)(1-\beta_1^2)}} \left( -\beta_2 - \frac{z(1-\beta_2^2)}{\sqrt{(1-z^2)(1-\beta_2^2)}} \right) \right. \\
&- \left. \frac{1-z\beta_2 + \sqrt{(1-z^2)(1-\beta_2^2)}}{(1-z\beta_1 + \sqrt{(1-z^2)(1-\beta_1^2)})^2} \left( -\beta_1 - \frac{z(1-\beta_1^2)}{\sqrt{(1-z^2)(1-\beta_1^2)}} \right) \right] \\
&+ \frac{1}{1-z^2} \ln \left( \frac{1-z\beta_2 + \sqrt{(1-z^2)(1-\beta_2^2)}}{1-z\beta_1 + \sqrt{(1-z^2)(1-\beta_1^2)}} \right) \\
&+ \frac{(1-z\beta_1 + \sqrt{(1-z^2)(1-\beta_1^2)})}{(1-z\beta_2 + \sqrt{(1-z^2)(1-\beta_2^2)})} \left[ \frac{1}{1-z\beta_1 + \sqrt{(1-z^2)(1-\beta_1^2)}} \right. \\
&\times \left( -\frac{z^2(1-\beta_2^2)^2}{((1-z^2)(1-\beta_2^2))^{3/2}} - \frac{1-\beta_2^2}{\sqrt{(1-z^2)(1-\beta_2^2)}} \right) \\
&- 2 \frac{1}{(1-z\beta_1 + \sqrt{(1-z^2)(1-\beta_1^2)})^2} \left( -\beta_2 - \frac{z(1-\beta_2^2)}{\sqrt{(1-z^2)(1-\beta_2^2)}} \right) \\
&\times \left( -\beta_1 - \frac{z(1-\beta_1^2)}{\sqrt{(1-z^2)(1-\beta_1^2)}} \right) + 2 \frac{1-z\beta_2 + \sqrt{(1-z^2)(1-\beta_2^2)}}{(1-z\beta_1 + \sqrt{(1-z^2)(1-\beta_1^2)})^3} \\
&\times \left( -\beta_1 - \frac{z(1-\beta_1^2)}{\sqrt{(1-z^2)(1-\beta_1^2)}} \right)^2 - \frac{1-z\beta_2 + \sqrt{(1-z^2)(1-\beta_2^2)}}{(1-z\beta_1 + \sqrt{(1-z^2)(1-\beta_1^2)})^2} \\
&\times \left( -\frac{z^2(1-\beta_1^2)^2}{((1-z^2)(1-\beta_1^2))^{3/2}} - \frac{1-\beta_1^2}{\sqrt{(1-z^2)(1-\beta_1^2)}} \right) \left. \right\} \\
&- \frac{(1-z\beta_1 + \sqrt{(1-z^2)(1-\beta_1^2)})}{(1-z\beta_2 + \sqrt{(1-z^2)(1-\beta_2^2)})^2} \left[ \frac{1}{1-z\beta_1 + \sqrt{(1-z^2)(1-\beta_1^2)}} \right. \\
&\times \left( -\beta_2 - \frac{z(1-\beta_2^2)}{\sqrt{(1-z^2)(1-\beta_2^2)}} \right) - \frac{1-z\beta_2 + \sqrt{(1-z^2)(1-\beta_2^2)}}{(1-z\beta_1 + \sqrt{(1-z^2)(1-\beta_1^2)})^2} \\
&\times \left( -\beta_1 - \frac{z(1-\beta_1^2)}{\sqrt{(1-z^2)(1-\beta_1^2)}} \right) \left. \right] \left( -\beta_2 - \frac{z(1-\beta_2^2)}{\sqrt{(1-z^2)(1-\beta_2^2)}} \right) \\
&+ \frac{1}{(1-z\beta_2 + \sqrt{(1-z^2)(1-\beta_2^2)})} \left[ \frac{1}{1-z\beta_1 + \sqrt{(1-z^2)(1-\beta_1^2)}} \right. \\
&\times \left( -\beta_2 - \frac{z(1-\beta_2^2)}{\sqrt{(1-z^2)(1-\beta_2^2)}} \right) - \frac{1-z\beta_2 + \sqrt{(1-z^2)(1-\beta_2^2)}}{(1-z\beta_1 + \sqrt{(1-z^2)(1-\beta_1^2)})^2} \\
&\times \left( -\beta_1 - \frac{z(1-\beta_1^2)}{\sqrt{(1-z^2)(1-\beta_1^2)}} \right) \left. \right] \left( -\beta_1 - \frac{z(1-\beta_1^2)}{\sqrt{(1-z^2)(1-\beta_1^2)}} \right) \left. \right\}. \tag{B.13}
\end{aligned}$$



The last term is the derivative of the term similar to the RPDF. Its derivative is then of course similar. The derivative of the real part is

$$\begin{aligned} & \frac{\partial}{\partial z} \left[ -\frac{2gm}{1-z^2} e^{gf} \int_0^z d\zeta \frac{Q_1(mgR)}{R} \right] \\ &= \frac{2gm}{1-z^2} e^{gf} \left[ \frac{3z}{1-z^2} \int_0^z d\zeta \frac{mgR}{R} - \frac{gmz}{1-z^2} \int_0^z d\zeta Q_1'(mgR) - Q_1(mg) \right], \end{aligned} \quad (\text{B.14})$$

and the double derivative is

$$\begin{aligned} & \frac{\partial^2}{\partial z^2} \left[ -\frac{2gm}{1-z^2} e^{gf} \int_0^z d\zeta \frac{Q_1(mgR)}{R} \right] \\ &= \frac{2gm}{(1-z^2)^2} e^{gf} \left[ \frac{3(2z^2+1)}{1-z^2} \int_0^z d\zeta \frac{Q_1(mgR)}{R} - \frac{gm}{1-z^2} \int_0^z d\zeta Q_1'(mgR) \right. \\ & \quad \left. - \frac{g^2 m^2 z^2}{1-z^2} \int_0^z RQ_1''(mgR) + zQ_1(mg) - mgzQ_1'(mg) \right]. \end{aligned} \quad (\text{B.15})$$

For the imaginary part only the first derivative is needed. It is

$$\begin{aligned} & -i\pi \frac{\partial}{\partial z} [H(m\gamma_0 - a)b(m\gamma_0 - a)H(c - m\gamma_0) + H(m\gamma_0 - c)dH(f - m\gamma_0) \\ & \quad - H(m\gamma_0 - f)Ce^{-g(m\gamma - f)}H(h - m\gamma_0)] \\ &= -i\pi m z \gamma_0^3 [H(m\gamma_0 - a)bH(c - m\gamma_0) + H(m\gamma_0 - f)gCe^{-g(m\gamma_0 - f)}H(h - m\gamma_0)]. \end{aligned} \quad (\text{B.16})$$

### B.3 Derivatives of $I(z)$ for $z > 1$

Some of the derivatives of  $I(z)$  for  $z > 1$  is the same as for  $z < 1$  these are not included. The derivative of (7.15) for  $z > 1$  is

$$\begin{aligned} & \frac{\partial}{\partial z} \left[ -\frac{2gm}{1-z^2} e^{gf} \int_z^\infty d\zeta \frac{Q_1(mgR)}{R} \right] \\ &= -\frac{2gm}{1-z^2} e^{gf} \left[ \frac{3z}{1-z^2} \int_z^\infty d\zeta \frac{Q_1(mgR)}{R} - \frac{mgz}{1-z^2} \int_z^\infty d\zeta Q_1'(mgR) + Q_1(mg) \right], \end{aligned} \quad (\text{B.17})$$

and the double derivative is

$$\begin{aligned} & \frac{\partial^2}{\partial z^2} \left[ -\frac{2gm}{1-z^2} e^{gf} \int_z^\infty d\zeta \frac{Q_1(mgR)}{R} \right] \\ &= -\frac{2gm}{(1-z^2)^2} e^{gf} \left[ \frac{3(2z^2+1)}{1-z^2} \int_z^\infty d\zeta \frac{Q_1(mgR)}{R} - \frac{gm}{1-z^2} \int_z^\infty d\zeta Q_1'(mgR) \right. \\ & \quad \left. - \frac{m^2 g^2 z^2}{1-z^2} \int_z^\infty d\zeta RQ_1''(mgR) - zQ_1(mg) + mgzQ_1'(mg) \right]. \end{aligned} \quad (\text{B.18})$$

$I(z)$  contains one more part, not included in the last section, whose derivative is

$$\begin{aligned}
& \frac{\partial}{\partial z} \frac{bm}{\sqrt{z^2-1}} \left[ \arcsin \left( \frac{1-z\beta_2}{z-\beta_2} \right) - \arcsin \left( \frac{1-z\beta_1}{z-\beta_1} \right) \right] \\
&= -\frac{bm}{(z^2-1)^{3/2}} \left\{ \frac{z}{(z^2-1)} \left[ \arcsin \left( \frac{1-z\beta_2}{z-\beta_2} \right) - \arcsin \left( \frac{1-z\beta_1}{z-\beta_1} \right) \right] \right. \\
&+ \left[ \left( \frac{\beta_2}{z-\beta_2} + \frac{1-z\beta_2}{(z-\beta_2)^2} \right) \frac{1}{\sqrt{1-\frac{(1-z\beta_2)^2}{(z-\beta_2)^2}}} \right. \\
&\left. \left. - \left( \frac{\beta_1}{z-\beta_1} + \frac{1-z\beta_1}{(z-\beta_1)^2} \right) \frac{1}{\sqrt{1-\frac{(1-z\beta_1)^2}{(z-\beta_1)^2}}} \right] \right\}, \tag{B.19}
\end{aligned}$$

and double derivative is

$$\begin{aligned}
& \frac{\partial^2}{\partial z^2} \frac{bm}{\sqrt{z^2-1}} \left[ \arcsin \left( \frac{1-z\beta_2}{z-\beta_2} \right) - \arcsin \left( \frac{1-z\beta_1}{z-\beta_1} \right) \right] \\
&= \frac{bm}{\sqrt{z^2-1}} \left\{ 3 \frac{z^2}{(z^2-1)^2} \left[ \arcsin \left( \frac{1-z\beta_2}{z-\beta_2} \right) - \arcsin \left( \frac{1-z\beta_1}{z-\beta_1} \right) \right] \right. \\
&+ 2 \frac{z}{z^2-1} \left[ \left( \frac{\beta_2}{z-\beta_2} + \frac{1-z\beta_2}{(z-\beta_2)^2} \right) \frac{1}{\sqrt{1-\frac{(1-z\beta_2)^2}{(z-\beta_2)^2}}} \right. \\
&\left. - \left( \frac{\beta_1}{z-\beta_1} + \frac{1-z\beta_1}{(z-\beta_1)^2} \right) \frac{1}{\sqrt{1-\frac{(1-z\beta_1)^2}{(z-\beta_1)^2}}} \right] \\
&- \frac{1}{z^2-1} \left[ \arcsin \left( \frac{1-z\beta_2}{z-\beta_2} \right) - \arcsin \left( \frac{1-z\beta_1}{z-\beta_1} \right) \right] \\
&+ \left[ \left( 2 \frac{\beta_2}{(z-\beta_2)^2} + 2 \frac{1-z\beta_2}{(z-\beta_2)^3} \right) \frac{1}{\sqrt{1-\frac{(1-z\beta_2)^2}{(z-\beta_2)^2}}} \right. \\
&\times \frac{1}{2} \left( \frac{\beta_2}{z-\beta_2} + \frac{1-z\beta_2}{(z-\beta_2)^2} \right) \left( 2 \frac{(1-z\beta_2)\beta_2}{(z-\beta_2)^2} + 2 \frac{(1-z\beta_2)^2}{(z-\beta_2)^3} \right) \\
&\times \left( 1 - \frac{(1-z\beta_2)^2}{(z-\beta_2)^2} \right)^{-3/2} - \left( 2 \frac{\beta_1}{(z-\beta_1)^2} + 2 \frac{1-z\beta_1}{(z-\beta_1)^3} \right) \frac{1}{\sqrt{1-\frac{(1-z\beta_1)^2}{(z-\beta_1)^2}}} \\
&- \frac{1}{2} \left( \frac{\beta_1}{z-\beta_1} + \frac{1-z\beta_1}{(z-\beta_1)^2} \right) \left( 2 \frac{(1-z\beta_1)\beta_1}{(z-\beta_1)^2} + 2 \frac{(1-z\beta_1)^2}{(z-\beta_1)^3} \right) \\
&\left. \times \left( -\frac{(1-z\beta_1)^2}{(z-\beta_1)^2} + 1 \right)^{-3/2} \right] \left. \right\}. \tag{B.20}
\end{aligned}$$

# Bibliography

- [1] M. Supsar. “Plasma Effects on Fast Electron-Positron Pair Beams in Cosmic Voids”. PhD thesis. Ruhr University Bochum, 2014.
- [2] U. Menzler and R. Schlickeiser. “The reduction of distant blazars’ inverse Compton cascade emission by plasma instability induced beam plateauing”. In: *Monthly Notices of the Royal Astronomical Society* 448 (4 2015), pp. 3405–3413.
- [3] R. Schlickeiser, D Ibscher, and M. Supsar. “Plasma Effects on Fast Pair Beams in Cosmic Voids”. In: *The Astrophysical Journal* 758 (2 2012), p. 102.
- [4] R. Durrer and A. Neronov. “Cosmological magnetic fields: their generation, evolution and obseration”. In: *The Astronomy and Astrophysics Review* 21 (1 2013), p. 62.
- [5] Bradley M. Peterson. *An Introduction to Active Galactic Nuclei*. The Edinburgh Building, Cambridge CB2 2RU, United Kingdom: Cambridge University Press, 1997.
- [6] R. Gould and G. Schröder. “Opacity of the Universe to High-Energy Photons”. In: *Physical Review Letters* 16 (6 1966), pp. 252–254.
- [7] F. Aharonian, P. S. Coppi, and H. J. Voelk. “Very High Energy Gamma-Rays from AGN: Cascading on the Cosmic Background Radiation Fields and the Formation of Pair Halos”. In: *The Astrophysical Journal* 423 (1994).
- [8] A. Neronov and L. Vovk. “Evidence for Strong Extragalactic Magnetic Fields from Fermi Observations of TeV Blazars”. In: *Science* 328 (5974 2010), pp. 73–75.
- [9] F. Tavecchio et al. “Extreme TeV blazars and the intergalactic magnetic field”. In: *Monthly Notices of the Royal Astronomical Society* 414 (4 2011), pp. 3566–3576.
- [10] K. Dolag et al. “Lower Limit on the Filling Factor of Extragalactic Magnetic Fields”. In: *The Astrophysical Journal Letters* 727 (1 2011), p. L4.
- [11] C. D. Dermer et al. “Time Delay of Cascade Radiation for Tev Blazars and the Measurement of the Intergalactic Magnetic Field.” In: *The Astrophysical Journal Letters* 732 (2 2011), p. L21.
- [12] I. Vovk et al. “Fermi/LAT Observations of 1ES 0229+200: Implications for Extragalactic Magnetic Fields and Background Light”. In: *The Astrophysical Journal Letters* 747 (1 2012), p. L14.

- [13] P. Chang, A. E. Broderick, and C. Pfrommer. “The cosmological impact of luminous TeV blazars. I. Implications of plasma instabilities for the intergalactic magnetic field and extragalactic gamma-ray background”. In: *The Astrophysical Journal* 752 (1 2012).
- [14] Donald B. Melrose. *Quantum Plasma Dynamics: Unmagnetized Plasmas*. New York: Springer, 2008.
- [15] E. Braaten and D. Segel. “Neutrino Energy Loss from the Plasma Process at All Temperature and Densities”. In: *Physical Review D* 48 (4 1993), p. 1478.
- [16] Volker Schönfelder. *The Universe in Gamma Rays*. New York: Springer, 2001.
- [17] C. Urry and P. Padovani. “Unified Schemes for Radio-Loud Active Galactic Nuclei”. In: *Publications of the Astronomical Society of the Pacific* 107 (1995), pp. 803–845.
- [18] National Institute of Technology and Standards. *Thomson Cross Section*. <https://physics.nist.gov/cgi-bin/cuu/Value?sigmae>. Online; accessed 28. February 2018.
- [19] Rudolf A. Treumann and Wolfgang Baumjohann. *Basic Space Plasma Physics*. London: Imperial College Press, 1996.
- [20] Rudolf A. Treumann and Wolfgang Baumjohann. *Advanced Space Plasma Physics*. London: Imperial College Press, 2001.
- [21] H. Walden. “Covariant calculations at finite temperature: The relativistic plasma”. In: *Physical Review Journal D* 26 (6 1982).
- [22] M. Kachelriess, S. Ostapchenko, and R. Thomás. “ELMAG: A Monte Carlo simulation of electromagnetic cascades on the extragalactic background light and in magnetic fields”. In: *Computer Physics Communications* 183 (4 2012), pp. 1036–1043.
- [23] D Verscharen et al. *ALPS: The Arbitrary Linear Plasma Solver*. arXiv:1803.04697, 2018.
- [24] G.N. Watson. *A Treatise on the Theory of Bessel Functions*. London: Cambridge University Press, 1966.